Title: Escape from recognition of SARS-CoV-2 Beta variant spike epitopes but overall preservation of T cell immunity

Catherine Riou[1,2,3,*], Roanne Keeton[2,3], Thandeka Moyo-Gwete[4,5], Tandile Hermanus[4,5], Prudence Kgagudi[4,5], Richard Baguma[2,3], Ziyaad Valley-Omar[3], Mikhail Smith[3], Houriiyah Tegally[6], Deelan Doolabh[3], Arash Iranzadeh[3], Lynn Tyers[3], Hygon Mutavhatsindi[1,2], Marius B. Tincho[2,3], Ntombi Benede[2,3], Gert Marais[3,7], Lionel R. Chinhoyi[8,9], Mathilda Mennen[8,9], Sango Skelem[8,9], Elsa du Bruyn[1,8], Cari Stek[1,8,10], SA-CIN[†], Tulio de Oliveira[6], Carolyn Williamson[1,2,3], Penny L. Moore[4,5], Robert J. Wilkinson[1,2,8,10,11], Ntobeko A. B. Ntusi[1,8,9], Wendy A. Burgers[1,2,3,*]

[1]Wellcome Centre for Infectious Diseases Research in Africa, University of Cape Town; Observatory 7925, South Africa.
[2]Institute of Infectious Disease and Molecular Medicine, University of Cape Town; Observatory 7925, South Africa.
[3]Division of Medical Virology, Department of Pathology; University of Cape Town; Observatory 7925, South Africa.
[4]National Institute for Communicable Diseases of the National Health Laboratory Services; Johannesburg, South Africa.
[5]MRC Antibody Immunity Research Unit, School of Pathology, Faculty of Health Sciences, University of the Witwatersrand; Johannesburg, South Africa.
[6]KwaZulu-Natal Research Innovation and Sequencing Platform; Durban, South Africa.
[7]Groote Schuur Hospital Medical Virology Laboratory of the National Health Laboratory Service; Observatory 7925, South Africa.
[8]Department of Medicine, University of Cape Town and Groote Schuur Hospital; Observatory 7925, South Africa.
[9]Hatter Institute for Cardiovascular Research in Africa, Faculty of Health Sciences, University of Cape Town; Observatory 7925, South Africa.
[10]Department of Infectious Diseases, Imperial College London; W12 0NN, UK.
[11]The Francis Crick Institute; London, NW1 1AT, UK.

*Corresponding authors. Catherine Riou; email: c.r.riou@uct.ac.za; Wendy Burgers; email: wendy.burgers@uct.ac.za

[†]South African Cellular Immunology Network (SA-CIN) collaborators and affiliations are listed in the supplementary materials.

One Sentence Summary:

T cell immunity to SARS-CoV-2 Beta is preserved in spite of some loss of variant epitope recognition by CD4 T cells.

ABSTRACT

SARS-CoV-2 variants have emerged that escape neutralization and potentially impact vaccine efficacy. T cell responses play a role in protection from reinfection and severe disease, but the potential for spike mutations to affect T cell immunity is incompletely understood. We assessed neutralizing antibody and T cell responses in 44 South African COVID-19 patients infected either with the Beta variant (dominant from November 2020 to May 2021) or infected prior to its emergence (first wave, Wuhan strain), to provide an overall measure of immune evasion. We show that robust spike-specific CD4 and CD8 T cell responses were detectable in Beta-infected patients, similar to first wave patients. Using peptides spanning the Beta-mutated regions, we identified CD4 T cell responses targeting the wild type peptides in 12/22 first wave patients, all of whom failed to recognize corresponding Beta-mutated peptides. However, responses to mutated regions formed only a small proportion (15.7%) of the overall CD4 response, and few patients (3/44) mounted CD8 responses that targeted the mutated regions. Among the spike epitopes tested, we identified three epitopes containing the D215, L18, or D80 residues that were specifically recognized by CD4 T cells, and their mutated versions were associated with a loss of response. This study shows that in spite of loss of recognition of immunogenic CD4 epitopes, CD4 and CD8 T cell responses to Beta are preserved overall. These observations may explain why several vaccines have retained the ability to protect against severe COVID-19 even with substantial loss of neutralizing antibody activity against Beta.

INTRODUCTION

High levels of ongoing SARS-CoV-2 transmission have led to the emergence of successive new viral variants, which now dominate the pandemic. Variants of concern have been characterized as having increased transmissibility, potentially greater pathogenicity, and the ability to evade host immunity *(1)*. Five such variants of concern have circulated around the world, namely Alpha, Beta, Gamma, Delta, the latter widely replacing many other variants, and more recently Omicron *(2–7)*. A primary concern is whether the immune response generated against ancestral SARS-CoV-2 strains, upon which all approved first generation vaccines are based, still confers protection against variants. The potential threat of reduced vaccine efficacy has prompted swift action from vaccine manufacturers, and adapted vaccines based on other variants have been developed and tested in preclinical and clinical trials *(8, 9)*.

Before the recent emergence of the SARS-CoV-2 Delta variant, the Beta variant, which was first described in South Africa in October 2020 *(5)*, was responsible for >95% of infections in the country and has spread across much of southern Africa *(6)*. It was a concerning variant from an immunological perspective, demonstrating the greatest reduction in neutralization sensitivity to COVID-19 convalescent and vaccinee plasma *(10–15)*, as well as reduced vaccine efficacy *(16–18)*. However, some vaccines have still demonstrated high efficacy against severe COVID-19 after Beta infection *(19)*, suggesting that T cell immunity plays an important role in immune protection, and may mitigate the effect of reduced neutralizing antibody activity.

To date, efforts to characterize immune evasion by SARS-CoV-2 variants have focused mainly on their ability to escape neutralization *(10–15)*. There is limited data addressing whether SARS-CoV-2 variants can evade T cell immunity *(20–24)* in natural infection or after vaccination. Furthermore, spike-specific T cell responses in COVID-19 patients infected with variant lineages have not been investigated. Here, we determined whether Beta spike mutations affect the recognition of T cell epitopes in patients infected with the ancestral or Beta SARS-CoV-2 lineages. We demonstrate that loss of CD4 T cell recognition does indeed occur in Beta-mutated spike regions, although the majority of the T cell response is maintained. Furthermore, Beta-infected patients mounted comparable spike responses as those infected with earlier strains. These results have important implications for reinfection and vaccine efficacy.

RESULTS

T cell responses in patients infected with ancestral strains or Beta

SARS-CoV-2 spike-specific neutralizing antibody and T cell responses were measured in hospitalized COVID-19 patients enrolled at Groote Schuur Hospital (Western Cape, South Africa) during the first wave of the COVID-19 pandemic (n = 22), prior to the emergence of the Beta variant, and during the second wave of the pandemic (n = 22), after the Beta variant became the dominant lineage (**Fig. 1A**). During the first wave, all sequenced virus corresponded to ancestral SARS-CoV-2 lineages (Wuhan and D614G). Conversely, during the second wave, the Beta lineage accounted for >95% of reported SARS-CoV-2 infections at the time of sample collection (**Fig. 1B)**. Beta is defined by nine amino acid changes in the spike protein, and all second wave participants that we sequenced (19/22) had confirmed infection with Beta and harbored 7 to 8 changes associated with the Beta lineage *(5)* (**Fig. S1**). Although SARS-CoV-2 viral sequences were not available for patients recruited in June to August 2020 during the first wave, we assumed that all participants were infected with a virus closely related to the ancestral virus, since Beta was first detected in October 2020 in the Western Cape.

First, we compared the magnitude of CD4 and CD8 T cell responses directed at the spike protein of SARS-CoV-2 in first and second wave patients. Using flow cytometry, we measured the production of IFN-γ, TNF-α or IL-2 in response to a peptide pool covering the full ancestral spike protein ('Full spike') (**Fig. 1C**). All participants tested exhibited a CD4 response, with a comparable frequency of spike specific-CD4 T cells in first and second wave patients ($P = 0.072$, **Fig. 1D**). A detectable spike CD8 response was observed in 63.6% (14/22) of first wave patients and 81.8% (18/22) of second wave patients ($P = 0.31$, Fisher's exact test). Amongst CD8 responders, the frequency of SARS-CoV-2 spike-specific CD8 T cell response was not significantly different between first and second wave patients ($P = 0.054$). As previously reported *(25)*, the magnitude of the SARS-CoV-2 spike-specific CD8 T cell response was significantly lower compared to the CD4 response in both first and second wave patients ($P = 0.0005$ and $P = 0.007$, respectively). Moreover, there were no significant differences in the frequency of SARS-CoV-2 spike-specific CD4 or CD8 T cells between patients with moderate or severe disease ($P = 0.3$ and $P = 0.36$, respectively). Also, no associations were found between the frequency of spike-specific CD4 or CD8 T cells and days post-PCR positivity ($P = 0.20$, r=

0.28 and $P = 0.1$, r = 0.24, respectively) or days since symptom onset in patients recruited during the first wave ($P = 0.22$, r = 0.28 and $P = 0.77$, r = 0.07, respectively). Lastly, the polyfunctional profiles of SARS-CoV-2 spike-specific CD4 or CD8 T cells were similar between first and second wave patients, with approximately one third of CD4 cells expressing at least two cytokines, while CD8 response was mostly IFN-γ monofunctional (**Fig. 1E and F**).

To ascertain whether similar patterns were maintained in convalescent COVID-19 donors, we compared the frequency of ancestral SARS-CoV-2 spike-, nucleocapsid (N)- and membrane (M)-specific CD4 and CD8 T cells in convalescent COVID-19 patients infected during the first wave with the ancestral strain (n = 10) or during the second wave, when Beta dominated (n = 14) (**Fig. 2A**). As for acute COVID-19 patients, the magnitude and polyfunctional profiles of ancestral SARS-CoV-2 spike-specific CD4 and CD8 T cell responses were comparable between convalescent individuals infected during the first or the second wave (**Fig. 2B, C and D**). Similar results were observed for CD4 responses against the SARS-CoV-2 N and M proteins (**Fig. 2B**). We also compared the profiles of spike-specific T cell responses cross-sectionally between acute and convalescent COVID-19 patients. Our data show that the frequency of spike-specific CD4 T cells is significantly lower in convalescent compared to acutely infected patients, regardless of the infecting strains ($P = 0.03$ for WT and $P < 0.0001$ for Beta) (**Fig. S2A**), which is likely related to the contraction of antigen-specific responses following viral clearance *(26)*. For spike-specific CD8 T cell responses, a lower frequency was observed only between acute and convalescent patients from the second wave ($P = 0.034$). Lastly, an increase in the polyfunctional profile of both spike-specific CD4 and CD8 T cells was observed in convalescent COVID-19 patients compared to those in the acute phase of infection, characterized by a substantial increase in IFN-γ, TNF-α and IL-2 co-expressing cells for spike-specific CD4 T cells and a significant reduction of IFN-γ monofunctional cells for spike-specific CD8 T cells (**Fig. S2B and C**). Overall, these data are in accordance with a recent report showing that T cell responses directed at the SARS-CoV-2 spike protein in convalescent COVID-19 donors infected with SARS-CoV-2 ancestral strain were not substantially affected by mutations found in SARS-CoV-2 variants *(24)*, and we further show that there is no overall dampening of T cell responses or change in functional profiles to the three immunogenic structural proteins of SARS-CoV-2 in those infected with Beta.

CD4 T cell targeting of variant spike epitopes

Since Beta-associated mutations occur only at a few residues of the spike protein, we assessed the recognition of peptide pools selectively spanning the variable regions of spike, one composed of the ancestral peptides ('WT pool') and the other Beta-mutated peptides ('Beta pool') (**Table S1**). Sample availability enabled us to perform these experiments in the acute COVID-19 cohort. Due to elevated TNF-α background observed in unstimulated cells (**Fig. 1C**), we focused on IFN-γ producing cells to measure T cell response to the smaller peptide pools. We previously described that acute COVID-19 patients had SARS-CoV-2-specific CD4 T cells characterized by elevated expression of PD-1 *(27)*. Thus, PD-1 was included in our flow cytometry panel to ensure that the phenotypic profile of CD4 T cells responding to the variable spike epitopes were consistent with our previous findings. In patients recruited during the first wave, IFN-γ CD4 T cell responses to the WT pool were detectable in 54.5% (12/22) patients (**Fig. 3A and B**). In those who mounted responses, the magnitude of the WT pool response was ~ 6.4-fold lower than full spike responses (median: 0.0075% vs 0.048%, respectively, $P < 0.0001$). In the 12 participants responding to the WT pool, the overall median relative contribution of WT epitopes located at spike mutation sites to the total spike-specific CD4 T cell response was 15.7%, ranging from 5.7% to 24%. This suggests that the majority of SARS-CoV-2 spike-specific CD4 T cell responses are directed against conserved epitopes between the ancestral and Beta lineage. When we tested the corresponding Beta pool, all 12 of the first wave WT pool responders failed to cross-react with the mutated peptides from Beta (**Fig. 3B,** left panel). These results show that Beta-mutated epitopes were no longer recognized by CD4 T cells targeting WT epitopes, demonstrating that this loss of recognition is likely mediated by variant mutations. This is broadly consistent with recent data from mRNA vaccinees, where full spike pools containing Beta mutated peptides detected T cell responses that were diminished by 30% compared to ancestral spike, revealing that the mutated sequences mediate differential recognition but make up a minor contribution to the overall spike-specific T cell response *(24)*.

We next measured peptide responses in patients infected with the Beta lineage. The Beta pool was not readily recognized by patients infected with the homologous variant (2/22; 9.1%) (**Fig. 3B,** right panel). A single donor had a detectable response to the WT but not Beta pool. These data suggest that mutations in Beta spike epitopes likely alter epitope binding to restricting

HLA molecules, consistent with the loss of recognition of Beta-mutated peptides by T cells in first wave patients.

In order to obtain an overall measure of immune escape in our participants, we measured their neutralizing antibody responses to the ancestral and Beta spike proteins (**Fig. 3C and D**). As we showed previously *(13),* in patients infected with the ancestral strains (first wave), a considerable loss of neutralization activity was observed against Beta (median fold change: 12.7, IQR: 7.3-18.8). In contrast, patients infected with Beta (second wave) retained a substantial capacity to neutralize ancestral virus, as shown by a moderate reduction in neutralizing activity (median: 2.3, IQR: 1.3-3.9). Of note, in the six first wave patients where loss of cross-neutralization was profound (titer <100), it is reassuring that the T cell response was relatively intact. We found no association between the frequency of SARS-CoV-2 spike-specific CD4 T cell responses and neutralizing activity (**Fig. S3A**), consistent with an earlier study *(28)*. Moreover, comparable frequencies of SARS-CoV-2-specific CD4 T cells were observed, irrespective of the extent of the loss of neutralizing activity against heterologous virus (**Fig. S3B**).

CD8 T cell targeting of variant spike epitopes

We next defined the recognition of WT and Beta peptide pools by CD8 T cells (**Fig. 4A**). Regardless of the infecting SARS-CoV-2 lineage, peptides covering the spike mutation sites were rarely recognized by CD8 T cells, with only 3/44 (6.8%) patients exhibiting a CD8 response, one in the first wave cohort and two in the second wave cohort. Thus, in contrast to CD4 T cells, the regions in which Beta mutations occur are not commonly targeted by CD8 T cells. Moreover, in these three patients, the frequency of IFN-γ-producing CD8 T cells was comparable between WT and Beta pool stimulation, indicating that mutations did not affect epitope recognition (**Fig. 4B**). Overall, these data indicate that Beta mutations do not affect CD8 T cell responses in our cohort.

Mapping of spike variable epitopes targeted by T cells

To gain deeper insight into the recognition of variable spike epitopes by CD4 cells in patients responding to the WT pool, responses to individual epitopes were measured in first wave COVID-19 patients (**Fig. 5A**). Amongst the six tested patients, a response to the spike 206-225

region (containing D215) was observed in 5 out of 6 patients, two of which also displayed a response to spike 6-25 region (containing L18). Moreover, a response towards the spike 73-92 region (containing D80) was detected in one participant (**Fig. 5B**). Mutation of these regions (L18F, D80A and D215G) resulted in a loss of CD4 response (**Fig. 3B** and **Fig. 5A**). No CD4 T cell responses to epitopes containing the K417, E484, N501 or A701 residues were observed (**Fig. 5B** and **C**).

To identify the potential HLA restriction associated with the recognition of the L18, D80 and D215 epitopes, predicted HLA class II restriction for each epitope was defined *in silico* (**Table S2**) and compared to HLA class II molecules expressed in our study cohort (**Table S3**). We identified that the D215 epitope was restricted by DRB1*03:01, DRB1*03:02 or DRB1*13:01; and the D215G mutation is predicted to be associated with a loss of response in those three alleles (**Data file S1**), as previously reported *(29)*. Nine first wave patients carried one of these alleles, eight of whom exhibited a response to the D215 epitopes (n = 5) or the WT pool (n = 3). No matching alleles were predicted for the L18 and D80 epitopes, despite CD4 responses to the spike regions 6-20, 11-25 and 78-92 having been previously reported previously *(30, 31)*.

Due to limited availability of samples, we could not test all WT pool responders for single epitope responses. However, based on predicted HLA class II restriction, we hypothesized that the peptide ^{236}TRFQTLLALH<u>R</u>SYLT^{250} (WT version of the 242-244del/R246I) may be an immunogenetic epitope, as previously described *(30, 32, 33)* restricted by DRB1*15:01, DRB1*15:03, DRB1*01:01 or DRB1*14:25 (**Table S4**). The 242-244del/R246I mutation is predicted to be associated with a loss of response to three of those alleles (DRB1*15:01, DRB1*15:03, and DRB1*14:25), while DRB1*01:01 retains its ability to bind the Beta-mutated epitope (^{236}TRFQTLH<u>I</u>SYLTPGD^{250}, 242-244del/R246I) based on the predicted IC50 and percentile rank value (**Data file S1**). Of note, 4 out of 6 alleles of interest (DRB1*03:01, DRB1*03:02, DRB1*13:01, DRB1*15:01, DRB1*15:03) exhibited comparable frequency distributions in first and second wave patients, while DRB1*01:01 and DRB1*14:25 were identified in only two patients from wave 1 (**Data file S2**). Of note, in first wave patients who did not mount a response to the WT pool (n = 10 out of 22, **Fig. 4B**), only two expressed an HLA-DRB1 allele associated with the recognition of the D215 or R246 epitopes. The absence of

response in these two donors could be due to the limited sensitivity of the flow cytometry assay used to measure T cell responses in this study.

In patients infected with Beta, three individuals exhibited a response to the WT pool, two of whom also responded to the Beta pool. Based solely on *in silico* predicted HLA class II restriction analysis, it was not possible to infer potential targeted peptides, as no specific epitopes could be associated with the HLA class II alleles carried by these patients. Of note, the viral sequence of all three did not have the L18A mutation (maintaining a lysine in position 18, characteristic of the WT strain). Additionally, in one of these responders, no D215G substitution was observed, but this specific individual did not carry any of the alleles associated with the recognition of the D215-containing epitope (**Table S4)**.

Regarding specific spike epitopes recognized by CD8 T cells, only three individuals exhibited a CD8 T cell response to the WT pool and comparable responses were obtained with the Beta pool (**Fig. 4**). All epitopes were tested *in silico* for predictive binding to HLA class I variants (HLA-A and HLA-B) expressed in the cohort (**Table S5**). The epitope ^{84}LPFNDGVYF^{92} showed the highest ranking for HLA-B*53:01, HLA-B*35:05 and HLA-B*35:30. Since CD8 responding participants carried the HLA-B*53:01 (SA2-016) or HLA-B*35:05 (SA1-098 and SA2-084) allele (**Data file S3**), this strongly suggests that the ^{84}LPFNDGVYF^{92} epitope is recognized by those participants. This confirms results reported by Tarke et al. *(31)* and further demonstrates that ^{84}LPFNDGVYF^{92} is also restricted by HLA-B*35:05. Moreover, as this predicted 9mer epitope is conserved between the ancestral strain and Beta variant and does not include the beta-mutated residue (D80A), it is unsurprising that the observed CD8 response is comparable when stimulation is performed using the WT or the Beta pool. Finally, these two alleles (B*53:01 and HLA-B*35:05) were found in only four participants (**Table S5**), three of whom exhibited a CD8 response to the WT and Beta pool.

DISCUSSION

We demonstrate that infection with the Beta variant results in robust T cell responses, comparable to responses elicited to ancestral strains. We also demonstrate that the recognition of epitopes by CD4 T cells targeting variable spike regions is affected by Beta spike mutations in patients infected with ancestral lineages. However, the loss of recognition of Beta mutated spike epitopes had a minor impact on the overall CD4 Th1 cell response. Moreover, CD8 T cell responses to spike were unaffected by mutations in Beta.

We focused our analysis on spike, because specific mutations or deletions within or outside of T cell epitopes can lead to lack of cross-recognition, or loss of presentation, and may have important implications for vaccine protection. However, recent studies have revealed a more global strategy employed by SARS-CoV-2 variants to potentially evade immunity. The suppression of innate immune responses was demonstrated for the Alpha variant, as well as interferon resistance *in vitro (34, 35)*. Thus, given the possibility that variant mutations may have broader effects on adaptive responses, we also examined T cell responses to other dominant targets, namely the nucleocapsid and membrane proteins *(26, 28, 31, 36)*. We detected similar T cell response frequencies between first and second wave convalescent donors for both CD4 and CD8 T cells, irrespective of the SARS-CoV-2 protein examined, suggesting that there was not a general dampening of T cell responses to Beta. Altogether, we confirm that infection with Beta does not significantly affect the overall recognition or functional profile of T cell responses to the ancestral virus in either acute or chronic infection.

It is of interest to determine whether specific mutations in SARS-CoV-2 variants may lead to evasion of cellular immunity, as has been demonstrated for neutralizing antibodies. Having demonstrated that ancestral versions of peptides mutated in Beta were targeted by CD4 T cells from first wave participants, and there was a loss of recognition of the Beta peptides, we reasoned that one or more epitopes in the Beta pool may be affected by variant mutations. We identified three epitopes containing the D215, L18, or D80 residues that were specifically recognized by CD4 T cells, and mutated versions in Beta were associated with a loss of response. HLA genotyping revealed the predicted MHC class II alleles restricting the D215 epitope, and *in silico* analyses confirmed that mutations would no longer be restricted by those alleles. This provides important information regarding mutations occurring in SARS-CoV-2 variants, the

predicted epitopes within which they are located, immune evasion properties associated with them, and their restricting alleles. Of note, the L18F mutation is of importance as it is a frequently observed mutation, with a 4% cumulative prevalence in all SARS-CoV-2 sequences in GISAID *(37),* present in Gamma and in a number of other lineages, in particular B.1.177 that circulated widely in Europe *(38)*. L18F is expected to have a detrimental impact on antibody binding, thus the mutation could result from selective pressure from both antibodies and T cells. D215, located in the epitope most frequently targeted by first wave patients of the three epitopes we identified, is mutated to G in Beta, which is shared by the C.1.2 variant *(39)*, a highly mutated variant under monitoring, as well as B.1.616 and AT.1 lineages, all of which occur at frequencies <0.5% worldwide *(40)*. These observations further underscore the limited impact these mutations may have on the CD4 T cell response at a global level.

We were unable to confirm class II HLA restriction of the peptides containing the L18 and D80 residues, with the predicted HLA molecules for the L18 epitope not matching those expressed in our cohort, and no restricting alleles predicted for the D80-containing peptide. Epitopes containing these residues have been described in other studies, without presenting HLA restriction *(30, 31)*.This is likely due to the limited accuracy of Class II prediction algorithms. An additional CD4 epitope containing the R246 residue is a likely target for which HLA binding is abrogated in the Beta variant for particular Class II alleles, and may have also contributed to targeting of the WT pool. However, limited cell availability prevented us from experimentally confirming the targeting of this epitope in our cohort, but several studies have confirmed targeting of this region *(30, 32, 33)*.

We found that spike-specific CD8 responses were not affected by mutations in Beta in our cohort. A single epitope (residues 84-94 of spike) was predicted to account for the CD8 response to the WT or Beta pool in three individuals in the cohort. Consistent with the recognition of both WT and mutated pools, the mutation fell outside the core binding motif for the predicted restricting Class I HLA molecules expressed by these donors. Overall, our results emphasize that the HLA repertoire in individuals determined whether they were impacted by mutations in variant epitopes, rather than the mutated epitopes dictating population-wide effects, as observed with certain key neutralizing antibody epitopes in variants of concern. These observations further emphasise that HLA polymorphism will likely limit the impact of T cell escape on SARS-CoV-2 immunity to viral variants. Two possible scenarios could change this: 1)

the mutation of dominant epitopes *(32)* or those broadly restricted ('promiscuous epitopes') by multiple commonly-expressed alleles *(29)*, or 2) if accumulation of mutations associated with T cell evasion occurs in variants. To date, neither of these have occurred.

This work extends our recent findings characterizing neutralizing antibody responses elicited by Beta *(13, 41)*. Neutralization resistance for Beta, Gamma and Delta confers the ability to evade antibodies after infection and vaccination, to varying degrees *(11, 42–44)*. Beta is approximately 10-fold more resistant to convalescent plasma and sera from vaccinated individuals than ancestral SARS-CoV-2 *(14, 15, 45)*. Comparative analyses of SARS-CoV-2 variants demonstrated that Beta is the most refractory to neutralization of all the VOC that have emerged to date (*12*, *46, 47*), however early indications are that Omicron will result in greater escape from neutralization *(48)*.

Recent studies examining vaccine-induced neutralizing antibodies (nAb) and vaccine efficacy demonstrate that nAb titers are a correlate of protection *(49, 50)*. The demonstration of an antibody correlate does not preclude a contribution from other immune components for protection. CD4 T cell responses are required for strong Ab responses, and CD8 T cells play an important role in the context of sub-optimal antibody titers in a macaque model *(51)*. Multiple mechanisms, involving nAb, CD4 and CD8 T cells acting in a coordinated manner appear to effectively control established infection *(52)*.

In contrast to neutralizing antibody epitopes, T cell epitopes are abundantly located across the spike protein *(30, 31, 53–55)*. Regions in spike most frequently targeted by CD4 T cells are the N-terminal domain of both the S1 and S2 subunits, with the receptor binding domain (RBD) being relatively epitope-poor *(31)*. This is consistent with the three CD4 epitopes we identified in this study. In contrast, CD8 T cell epitopes are broadly distributed across spike *(31, 53)*. Sustained efforts to map epitopes in spike, particularly in a range of populations encompassing greater HLA diversity will be beneficial for evaluating the effect on T cell immunity for mutations that may arise in future VOC. Thus, it is unsurprising that Beta retains the ability to generate strong T cell immune responses, as Beta spike mutations are limited to a few residues.

Viral evasion of cytotoxic T lymphocyte or T helper recognition may result in delayed clearance of infected cells, or inadequate help provided to B cells, influencing the antibody response. Viral escape from specific SARS-CoV-2 CD8 epitopes has recently been described, in

spike, nucleocapsid and ORF3a *(20, 21, 23)*. Both CD4 and CD8 T cells can exert selective pressure on viruses resulting in mutational escape, thereby driving viral evolution. In addition to their role in supporting the maturation of B cells and CD8 T cell responses, CD4 T cells may play additional antiviral roles, including directly lysing infected cells *(56)*. Indeed, transcriptomic profiles of SARS-CoV-2-specific CD4 T cells demonstrated a subset expressing transcripts for cytotoxic molecules *(57)*. Abundant populations of cytotoxic CD4 have been described in the lungs in COVID-19 patients *(58)*, where they may participate in viral clearance. In addition to direct selective pressure, mutations occurring in response to immune pressure from neutralizing antibodies or associated with increased viral infectivity *(23)* could coincide with T cell epitopes, thus representing 'collateral damage' for the T cell response.

Our study had several limitations. Although convenient for mapping approaches, it has been demonstrated that 15mer peptides are not optimal for all HLA class I-restricted T cells *(59)*. Approaches using optimal CD8 epitopes *(25, 53)* may have yielded greater sensitivity to detect CD8 responses. Furthermore, examining responses to Beta in the context of full mutated spike *(22, 24)* would corroborate our findings regarding the degree to which the overall spike T cell response is affected by mutations.

In conclusion, although Beta no longer has significant prevalence compared to Delta and the highly mutated Omicron in residues that are key for antibody recognition, these results are relevant in advancing our understanding of the cross-reactive potential of T cell immunity in the context of viral variability and highlight the importance of monitoring both antibody and T cell responses to emerging SARS-CoV-2 variants. We demonstrate a limited effect of viral mutations on T cell immunity which may explain why, despite substantial loss of neutralizing antibody activity against Beta and Delta, vaccines have retained the ability to protect against severe COVID-19. We and others have shown that vaccine-induced T cell immunity effectively recognizes SARS-CoV-2 variants *(24, 60–63)*. Whilst second generation vaccines based on SARS-CoV-2 variants are desirable, they may not be needed to generate improved T cell responses.

MATERIALS AND METHODS

Study Design

Hospitalized patients with PCR-confirmed acute COVID-19 were enrolled at Groote Schuur Hospital (Cape Town, Western Cape, South Africa) between June 11th and August 21st, 2020 (first wave, n = 22) and between December 31st, 2020 and January 15th, 2021 (second wave, n = 22). The clinical characteristics of participants are summarized in **Fig. 1A**. Clinical folders were consulted for all second wave patients and none showed evidence of prior symptomatic COVID-19. Blood samples were obtained a median of 4.5 days [interquartile range (IQR): 3-7] after a positive PCR test for SARS-CoV-2 for first wave patients, and 8 days [IQR: 4-16] for second wave patients. Viral sequences were available for 19/22 second wave participants (**Fig. S1**). T cell responses were assessed by stimulating PBMC with peptide pools spanning full-length spike or smaller pools covering the regions mutated in Beta, followed by intracellular cytokine staining and flow cytometry (**Fig. S4**). Additionally, convalescent COVID-19 patients infected with the ancestral SARS-CoV-2 strain or Beta were included in this study. Samples were obtained a median of 98 days [IQR: 79-110] after a positive PCR test for first wave participants, and 67 days [IQR: 54-105] for second wave participants (**Fig. S2A).** The study was approved by the University of Cape Town Human Research Ethics Committee (HREC: 207/2020 and R021/2020) and written informed consent was obtained from all participants.

SARS-CoV-2 spike whole genome sequencing

Whole genome sequencing of SARS-CoV-2 was performed using nasopharyngeal swabs obtained from 19 of the hospitalized patients recruited during the second wave. Sequencing was performed as previously published *(41)*. Briefly, cDNA was synthesized from RNA extracted from swabs using the Superscript IV First Strand synthesis system (Life Technologies) and random hexamer primers. Whole genome amplification was performed by multiplex PCR using the ARTIC V3 protocol (https://www.protocols.io/view/ ncov-2019-sequencing-protocol-v3-locost-bh42j8ye). PCR products were purified with AMPure XP magnetic beads (Beckman Coulter) and quantified using the Qubit dsDNA High Sensitivity assay on the Qubit 3.0 instrument (Life Technologies). The Illumina® DNA Prep kit was used to prepare indexed paired end libraries of genomic DNA. Sequencing libraries were normalized to 4

nM, pooled, and denatured with 0.2 N sodium hydroxide. Libraries were sequenced on the Illumina MiSeq instrument. The quality control checks on raw sequence data and the genome assembly were performed using Genome Detective 1.132 (https://www.genomedetective.com) and the Coronavirus Typing Tool *(64)*. The initial assembly was polished by aligning mapped reads to the references and filtering out low-quality mutations using bcftools 1.7-2 mpileup method. Mutations were confirmed visually with bam files using Geneious software (Biomatters Ltd). Phylogenetic clade classification of the genomes in this study consisted of analyzing them against a global reference dataset using a custom pipeline based on a local version of NextStrain (https://github.com/nextstrain/ncov) *(65)*. The workflow performs alignment of genomes, phylogenetic tree inference, tree dating and ancestral state construction and annotation. Phylogenetic trees were visualized using ggplot and ggtree *(66)*. GISAID accession numbers are as follows: EPI_ISL_1040644, 1040645, 1040646, 1040650, 1040654, 1040656, 1040659, 1040672, 1040683, 1040692, 1040696, 1040697, 1040698, 1040707, 1040714, 1040716, 1040754, 1040758, 1534362.

Ancestral (wild type) and Beta variant SARS-CoV-2 peptides

To assess the response to the full length SARS-CoV-2 spike protein, we combined two commercially available peptide pools (PepTivator®, Miltenyi Biotech) including: i) a pool of peptides (15mers with 11 aa overlap) covering the ancestral N-terminal S1 domain of SARS-CoV-2 (GenBank MN908947.3, Protein QHD43416.1) from aa 1 to 692 and ii) a pool of peptides(15mers with 11 aa overlap) covering the immunodominant sequence domains of the ancestral C-terminal S2 domain of SARS-CoV-2 (GenBank MN908947.3, Protein QHD43416.1) including aa 683-707, aa 741-770, aa 785-802, and aa 885-1273. Pools were resuspended in distilled water at 50 µg/mL. Individual peptides (15mers with 11 aa overlap) spanning ancestral or Beta spike mutation sites (L18F, D80A, D215G, del 242-244, R246I, K417N, E484K, N501Y and A701V) were synthesized (GenScript) and individually resuspended in dimethyl sulfoxide (DMSO; Sigma-Aldrich) at 20 µg/mL. Peptide sequences are provided in **Table S1**, which also indicates where their recognition has been previously described *(30, 31, 55)*. Ancestral or Beta pools (16 peptides) selectively spanning the mutated regions were created by pooling aliquots of these individual peptides at a final concentration of 160 µg/mL. To assess T cell responses to SARS-CoV-2 nucleocapsid and membrane proteins, commercially available peptide pools

(15mers with 11 aa overlap, PepTivator®, Miltenyi) covering the complete sequence of the SARS-CoV-2 membrane glycoprotein (M, GenBank MN908947.3, Protein QHD43419.1) or nucleocapsid (N, GenBank MN908947.3, Protein QHD43423.2) were used.

Isolation of peripheral blood mononuclear cells (PBMC)

Blood was collected in heparin tubes and processed within 3 hours. PBMC were isolated by density gradient sedimentation using Ficoll-Paque (Amersham Biosciences) as per the manufacturer's instructions and cryopreserved in freezing media consisting of heat-inactivated fetal bovine serum (FBS, Thermo Fisher Scientific) containing 10% DMSO and stored in liquid nitrogen.

Cell stimulation and flow cytometry staining

Cryopreserved PBMC were thawed, washed and rested in RPMI 1640 containing 10% heat-inactivated FBS for 4 hours. PBMC were seeded in a 96-well V-bottom plate at ~2 x 10^6 PBMC per well and stimulated with SARS-CoV-2 M or N peptide pools (4 µg/mL), SARS-CoV-2 spike peptide pools: full spike pool (4 µg/mL), and ancestral and Beta pools selectively spanning the mutated regions (4 µg/mL). All stimulations were performed in the presence of Brefeldin A (10 µg/mL, Sigma-Aldrich) and co-stimulatory antibodies against CD28 (clone 28.2) and CD49d (clone L25) (1 µg/mL each; BD Biosciences). As a negative control, PBMC were incubated with co-stimulatory antibodies, Brefeldin A and an equimolar amount of DMSO (0.15%).
After 16 hours of stimulation, cells were washed, stained with LIVE/DEAD™ Fixable Near-IR Stain (Invitrogen) and subsequently surface stained with the following antibodies: CD4 BV785 (OKT4, Biolegend), CD8 BV510 (RPA-8, Biolegend), PD-1 PE (J105, eBioscience). Cells were then fixed and permeabilized using a Transcription Factor Fixation buffer (eBioscience) and stained with CD3 BV650 (OKT3), IFN-γ BV711 (4S.B3), TNF-α PE-cy7 (MAB11) and IL-2 PE-Dazzle (MQ1-17H12) from Biolegend. Finally, cells were washed and fixed in 1% formaldehyde in PBS. Samples were acquired on a BD LSR-II flow cytometer and analyzed using FlowJo (v9.9.6, FlowJo LLC). The gating strategy is presented in **Fig. S5.** A cytokine response was defined as positive when the frequency of cytokine produced in stimulated wells was at least twice the background of unstimulated cells. All summary data are presented after

background subtraction. For the identification of specific spike epitopes, five acute COVID-19 patients and one convalescent donor were tested.

SARS-CoV-2 pseudovirus based neutralization assay

SARS-CoV-2 pseudotyped lentiviruses were prepared by co-transfecting the HEK 293T cell line with the SARS-CoV-2 614G spike (D614G) or SARS-CoV-2 Beta spike (L18F, D80A, D215G, K417N, E484K, N501Y, A701V, 242-244 del) plasmids with a firefly luciferase encoding lentivirus backbone plasmid. The parental plasmids were provided by Drs Elise Landais and Devin Sok (IAVI). For the neutralization assays, heat-inactivated plasma samples were incubated with SARS-CoV-2 pseudotyped virus for 1 hour at 37°C, 5% CO_2. Subsequently, $1x10^4$ HEK293T cells engineered to over-express ACE-2, provided by Dr Michael Farzan (Scripps Research Institute), were added and the incubated at 37°C, 5% CO_2 for 72 hours, upon which the luminescence of the luciferase gene was measured. CB6 and CA1 monoclonal antibodies were used as controls.

HLA typing

Genomic DNA was isolated from PBMC using standard techniques (Qiagen). Amplicons for class I (HLA-A, B and C) and II (DRB1, DQB1 and DPB1) HLA loci were generated using the NGSgo®-MX6-1 multiplex PCR (GenDX), according to the manufacturer's instructions. Sequencing libraries were prepared using the NGSgo-LibrX kit (GenDX), dual indexed using the NGSgo-IndX kit (GenDX) and pooled, according to the manufacturer's instructions. Pooled libraries were loaded at 12 pM on a MiSeq Micro flow cell (Illumina) and run using a MiSeq reagent kit V2 (Illumina). Paired-end sequencing was performed on the MiSeq NGS platform (Illumina), 151 cycles in each direction. HLA typing calls were made using the NGS-engine HLA typing software package (Version 2.22, GenDX) along with the 3.44.1 version of the IPD-IMGT/HLA database. HLA class II and class I genotypes are presented in **Table S3** and **Table S5**. The frequency distributions of HLA-DRB1, HLA-A and HLA-B alleles were comparable between patients recruited during first or second wave of the COVID-19 epidemic (**Data file S2**).

HLA class I and HLA class II binding prediction for T cell epitopes

Putative HLA restrictions were inferred using the Immune Epitope Database (IEDB, http://tools.iedb.org/main/). For HLA class I, all peptides included in the WT and Beta pools (**Table S1**) were submitted to Tepitool (http://tools.iedb.org/tepitool/) using the NetMHCpan method, including all HLA-A and HLA-B alleles identified in the study cohort (**Data file S2**). The epitopes that had a predicted IC50 > 50 nM were excluded and sequences ordered by percentile rank *(67)*. For class II, the same peptides were submitted to the IEDB MHC class II epitope prediction tool (http://tools.iedb.org/mhcii/) including all HLA-DP, DQ and DR alleles identified in the cohort (**Data file S1**). HLA class II binding predictions were performed using two methodologies: first, NetMHCIIpan 3.2 *(68, 69)* was used to extract IC50 predicted values, then the IEDB recommended 2.22 methodology (combining the comblib *(70)*, SMM *(71)*, NN *(68)* and Sturniolo *(72)* algorithms was used and rank percentile values were extracted. Only epitopes with a predicted IC50 < 500 nM and percentile rank ≤ 20 were selected.

Statistical analyses

Analyses were performed in Prism (v9; GraphPad). Non-parametric tests were used for all comparisons. The Mann-Whitney and Wilcoxon tests were used for unmatched and paired samples, respectively. *P* values less than 0.05 were considered to indicate statistical significance. All data used to compile figures can be found in **Data file S4**.

SUPPLEMENTARY MATERIALS

Fig. S1. Genomic sequencing confirmation of SARS-CoV-2 Beta infection of COVID-19 second wave patients.

Fig. S2. Comparison of the frequency and polyfunctionality of T cell response to ancestral SARS-CoV-2 spike protein between acute and convalescent COVID-19 patients.

Fig. S3. Relationship between SARS-CoV-2-specific CD4 T cell response and neutralizing activity in acute COVID-19 patients.

Fig. S4. Graphical representation of study approach.

Fig. S5. Flow cytometry gating strategy.

Table S1. Peptides included in the ancestral and Beta peptide pools.

Table S2. List of CD4+ T cell epitopes used in this study and their predicted HLA class II restriction(s).

Table S3. HLA class II genotype of COVID-19 patients.

Table S4. List of spike epitopes tested and their predicted HLA Class II restriction.

Table S5. HLA class I genotype of COVID-19 patients.

Data file S1. HLA class II binding prediction for the 16 peptides included in the WT or Beta pool

Data file S2. Prevalence of HLA-DRB1, HLA-A and HLA-B in patients recruited during first and second wave of the COVID-19 epidemic.

Data file S3. HLA class I binding prediction for the 16 peptides included in the WT or Beta pool

Data file S4. Raw data for each Figure.

REFERENCES AND NOTES

1. J. A. Plante, B. M. Mitchell, K. S. Plante, K. Debbink, S. C. Weaver, V. D. Menachery, The Variant Gambit: COVID's Next Move, *Cell Host Microbe* **29**, 508–515 (2021).
2. Centers for Disease Control and Prevention, 2021. https://covid.cdc.gov/covid-data-tracker/#datatracker-home. *Accessed 10 September 2021*.
3. European Centre for Disease Prevention and Control, 2021. https://www.ecdc.europa.eu/en/covid-19/variants-concern. *Accessed 10 September 2021*.
4. S. Cherian, V. Potdar, S. Jadhav, P. Yadav, N. Gupta, M. Das, P. Rakshit, S. Singh, P. Abraham, S. Panda, N. Team, SARS-CoV-2 Spike Mutations, L452R, T478K, E484Q and P681R, in the Second Wave of COVID-19 in Maharashtra, India, *Microorg* **9**, 1542 (2021).
5. H. Tegally, E. Wilkinson, M. Giovanetti, A. Iranzadeh, V. Fonseca, J. Giandhari, D. Doolabh, S. Pillay, E. J. San, N. Msomi, K. Mlisana, A. von Gottberg, S. Walaza, M. Allam, A. Ismail, T. Mohale, A. J. Glass, S. Engelbrecht, G. V. Zyl, W. Preiser, F. Petruccione, A. Sigal, D. Hardie, G. Marais, N. Hsiao, S. Korsman, M.-A. Davies, L. Tyers, I. Mudau, D. York, C. Maslo, D. Goedhals, S. Abrahams, O. Laguda-Akingba, A. Alisoltani-Dehkordi, A. Godzik, C. K. Wibmer, B. T. Sewell, J. Lourenço, L. C. J. Alcantara, S. L. K. Pond, S. Weaver, D. Martin, R. J. Lessells, J. N. Bhiman, C. Williamson, T. de Oliveira, Detection of a SARS-CoV-2 variant of concern in South Africa, *Nature* **592**, 438–443 (2021).
6. E. Wilkinson, M. Giovanetti, H. Tegally, J. E. San, R. Lessels, D. Cuadros, D. P. Martin, A.-R. N. Zekri, A. K. Sangare, A.-S. Ouedraogo, A. K. Sesay, A. Hammami, A. A. Amuri, A. Sayed, A. Rebai, A. Elargoubi, A. J. Trotter, A. K. Keita, A. A. Sall, A. Kone, A. Souissi, A. V. Gutierrez, A. J. Page, A. Iranzadeh, A. Lambisia, A. Sylverken, A. Ibrahimi, B. Dhaala, B. Kouriba, B. Kleinhans, C. Brook, C. Williamson, C. B. Pratt, C. G. Akoua-Koffi, C. N. Agoti, C. M. Morang'a, D. J. Nokes, D. J. Bridges, D. L. Bugembe, D. Baker, D. Doolabh, D. Ssemwanga, D. Tshabuila, D. Bassirou, D. S. Y. Amuzu, D. Goedhals, D. Maruapula, E. Foster-Nyarko, E. K. Lusamaki, E. Simulundu, E. Moraa, E. N. Ngabana, E. E. Fahime, E. Jacob, E. Lokilo, E. Mukantwari, E. Belarbi, E. Simon-Loriere, E. A. Anoh, F. Leendertz, F. Ajili, F. Wasfi, F. T. Takawira, F. Derrar, F. Bouzid, F. M. Muyembe, F. Tanser, G. K. Mbunsu, G. Thilliez, G. Kay, G. Githinji, G. van Zyl, G. A. Awandare, G. Schubert, G. P. Maphalala, H. C. Ranaivoson, H. Lemriss, H. Abe, H. H. Karray, H. Nansumba, H. A. Elgahzaly, H. Gumbo, I. Smeti, I. B. Ayed, I. B.-B. Boubaker, I. Gaaloul, I. Gazy, I. Ssewanyana, J. B. Lekana-Douk, J.-C. C. Makangara, J.-J. M. Tamfum, J.-M. Heraud, J. G. Shaffer, J. Giandhari, J. Li, J. Yasuda, J. Q. Mends, J. Kiconco, J. Morobe, J. N. Nkengasong, J. O. Gyapong, J. T. Kayiwa, J. A. Edwards, J. Gyamfi, J. Farah, J. M. Ngoi, J. Namulondo, J. C. Andeko, J. J. Lutwama, J. O'Grady, K. A. Tumedi, K. M. Said, K. Hae-Young, K. O. Duedu, L. Belyamani, L. Singh, L. de O. Martins, M. Mine, M. Ramuth, M. Mastouri, M. Aouni, M. el Hefnawi, M. I. Matsheka, M. Kebabonye, M. Turki, M. M. Nyaga, M. Mareka, M. Damaris, M. Cotten, M. W. Mburu, M. Mpina, M. Owusu, M. R. Wiley, M. A. Ali, M. Abouelhoda, M. G. Seadawy, M. K. Khalifa, M. Sekhele, M. Ouadghiri, M. Mwenda, M. Allam, M. V. T. Phan, N. Abid, N. Touil, N. Kharrat, N. Ismael, N. Mabunda, N. Hsiao, N. B. Silochi, N. Saasa, N. Mulder, P. Combe, P. Semanda, P. E. Oluniyi, P. Arnaldo, P. K. Quashie, P. A. Bester, P. Dussart, P. K. Mbala, P. Kaleebu, R. Ayivor-Djanie, R. Njouom, R. O. Phillips, R. Gorman, R. A. Kingsley, R. A. A. Carr, S. E. Kabbaj, S. Gargouri, S. Masmoudi, S. Kassim, S. Trabelsi, S. Kammoun, S. Lemriss, S. H. Agwa, S. Calvignac-Spencer, S. Doumbia, S. M. Mandanda, S. Aryeetey, S. S. Ahmed, S. Moyo, S. Gaseitsiwe, S.

Lekana-Douki, S. Prosolek, S. Ouangraoua, S. A. Mundeke, S. Rudder, S. Panji, S. Pillay, S. Engelbrecht, S. Nabadda, S. Behillil, S. L. Budiaki, S. van der Werf, T. Mashe, T. Aanniz, T. Mohale, T. Le-Viet, T. Schindler, U. J. Anyaneji, U. Ramphal, V. Fonseca, V. Enouf, V. Gorova, W. H. Roshdy, W. K. Ampofo, W. Preiser, W. T. Choga, Y. Bediako, Y. K. Tebeje, Y. Naidoo, Z. R. de Laurent, S. K. Tessema, T. de Oliveira, A year of genomic surveillance reveals how the SARS-CoV-2 pandemic unfolded in Africa, *Science* 10.1126/science.abj4336 (2021).

7. S. S. A. Karim, Q. A. Karim, Omicron SARS-CoV-2 variant: a new chapter in the COVID-19 pandemic. *Lancet* (2021), doi:10.1016/s0140-6736(21)02758-6.
8. A. J. Spencer, S. Morris, M. Ulaszewska, C. Powers, R. Kaliath, C. D. Bissett, A. Truby, N. Thakur, J. Newman, E. R. Allen, I. Rudiansyah, C. Lui, W. Dejnirattisai, J. Mongkolsapaya, H. Davies, F. R. Donnellan, D. Pulido, T. P. Peacock, W. S. Barclay, H. Bright, K. Ren, G. Screaton, P. McTammy, D. Bailey, S. C. Gilbert, T. Lambe, The ChAdOx1 vectored vaccine, AZD2816, induces strong immunogenicity against SARS-CoV-2 B.1.351 and other variants of concern in preclinical studies, *Biorxiv*, 2021.06.08.447308 (2021).
9. K. Wu, A. Choi, M. Koch, L. Ma, A. Hill, N. Nunna, W. Huang, J. Oestreicher, T. Colpitts, H. Bennett, H. Legault, Y. Paila, B. Nestorova, B. Ding, R. Pajon, J. M. Miller, B. Leav, A. Carfi, R. McPhee, D. K. Edwards, Preliminary Analysis of Safety and Immunogenicity of a SARS-CoV-2 Variant Vaccine Booster, *Medrxiv*, 2021.05.05.21256716 (2021).
10. S. Cele, I. Gazy, L. Jackson, S.-H. Hwa, H. Tegally, G. Lustig, J. Giandhari, S. Pillay, E. Wilkinson, Y. Naidoo, F. Karim, Y. Ganga, K. Khan, M. Bernstein, A. B. Balazs, B. I. Gosnell, W. Hanekom, M.-Y. S. Moosa, R. J. Lessells, T. de Oliveira, A. Sigal, Escape of SARS-CoV-2 501Y.V2 from neutralization by convalescent plasma, *Nature* **593**, 1–9 (2021).
11. R. E. Chen, X. Zhang, J. B. Case, E. S. Winkler, Y. Liu, L. A. VanBlargan, J. Liu, J. M. Errico, X. Xie, N. Suryadevara, P. Gilchuk, S. J. Zost, S. Tahan, L. Droit, J. S. Turner, W. Kim, A. J. Schmitz, M. Thapa, D. Wang, A. C. M. Boon, R. M. Presti, J. A. O'Halloran, A. H. J. Kim, P. Deepak, D. Pinto, D. H. Fremont, J. E. Crowe, D. Corti, H. W. Virgin, A. H. Ellebedy, P.-Y. Shi, M. S. Diamond, Resistance of SARS-CoV-2 variants to neutralization by monoclonal and serum-derived polyclonal antibodies, *Nat Med* **27**, 717–726 (2021).
12. W. F. Garcia-Beltran, E. C. Lam, K. St. Denis, A. D. Nitido, Z. H. Garcia, B. M. Hauser, J. Feldman, M. N. Pavlovic, D. J. Gregory, M. C. Poznansky, A. Sigal, A. G. Schmidt, A. J. Iafrate, V. Naranbhai, A. B. Balazs, Multiple SARS-CoV-2 variants escape neutralization by vaccine-induced humoral immunity, *Cell* **184**, 2523 (2021).
13. C. K. Wibmer, F. Ayres, T. Hermanus, M. Madzivhandila, P. Kgagudi, B. Oosthuysen, B. E. Lambson, T. de Oliveira, M. Vermeulen, K. van der Berg, T. Rossouw, M. Boswell, V. Ueckermann, S. Meiring, A. von Gottberg, C. Cohen, L. Morris, J. N. Bhiman, P. L. Moore, SARS-CoV-2 501Y.V2 escapes neutralization by South African COVID-19 donor plasma, *Nat Med* **27**, 622–625 (2021).
14. P. Wang, M. S. Nair, L. Liu, S. Iketani, Y. Luo, Y. Guo, M. Wang, J. Yu, B. Zhang, P. D. Kwong, B. S. Graham, J. R. Mascola, J. Y. Chang, M. T. Yin, M. Sobieszczyk, C. A. Kyratsous, L. Shapiro, Z. Sheng, Y. Huang, D. D. Ho, Antibody resistance of SARS-CoV-2 variants B.1.351 and B.1.1.7, *Nature* **593**, 1–6 (2021).
15. D. Zhou, W. Dejnirattisai, P. Supasa, C. Liu, A. J. Mentzer, H. M. Ginn, Y. Zhao, H. M. E. Duyvesteyn, A. Tuekprakhon, R. Nutalai, B. Wang, G. C. Paesen, C. Lopez-Camacho, J. Slon-Campos, B. Hallis, N. Coombes, K. Bewley, S. Charlton, T. S. Walter, D. Skelly, S. F. Lumley, C. Dold, R. Levin, T. Dong, A. J. Pollard, J. C. Knight, D. Crook, T. Lambe, E.

Clutterbuck, S. Bibi, A. Flaxman, M. Bittaye, S. Belij-Rammerstorfer, S. Gilbert, W. James, M. W. Carroll, P. Klenerman, E. Barnes, S. J. Dunachie, E. E. Fry, J. Mongkolspaya, J. Ren, D. I. Stuart, G. R. Screaton, Evidence of escape of SARS-CoV-2 variant B.1.351 from natural and vaccine induced sera, *Cell* **184**, 2348-2361.e6 (2021).

16. S. A. Madhi, V. Baillie, C. L. Cutland, M. Voysey, A. L. Koen, L. Fairlie, S. D. Padayachee, K. Dheda, S. L. Barnabas, Q. E. Bhorat, C. Briner, G. Kwatra, K. Ahmed, P. Aley, S. Bhikha, J. N. Bhiman, A. E. Bhorat, J. du Plessis, A. Esmail, M. Groenewald, E. Horne, S.-H. Hwa, A. Jose, T. Lambe, M. Laubscher, M. Malahleha, M. Masenya, M. Masilela, S. McKenzie, K. Molapo, A. Moultrie, S. Oelofse, F. Patel, S. Pillay, S. Rhead, H. Rodel, L. Rossouw, C. Taoushanis, H. Tegally, A. Thombrayil, S. van Eck, C. K. Wibmer, N. M. Durham, E. J. Kelly, T. L. Villafana, S. Gilbert, A. J. Pollard, T. de Oliveira, P. L. Moore, A. Sigal, A. Izu, N.-S. G. W. C. Group, Efficacy of the ChAdOx1 nCoV-19 Covid-19 Vaccine against the B.1.351 Variant, *New Engl J Med* **384**, 1185-1189 (2021).
17. J. Sadoff, G. Gray, A. Vandebosch, V. Cárdenas, G. Shukarev, B. Grinsztejn, P. A. Goepfert, C. Truyers, H. Fennema, B. Spiessens, K. Offergeld, G. Scheper, K. L. Taylor, M. L. Robb, J. Treanor, D. H. Barouch, J. Stoddard, M. F. Ryser, M. A. Marovich, K. M. Neuzil, L. Corey, N. Cauwenberghs, T. Tanner, K. Hardt, J. Ruiz-Guiñazú, M. L. Gars, H. Schuitemaker, J. V. Hoof, F. Struyf, M. Douoguih, E. S. Group, Safety and Efficacy of Single-Dose Ad26.COV2.S Vaccine against Covid-19, *New Engl J Med* **384**, 1824-1835 (2021).
18. V. Shinde, S. Bhikha, Z. Hoosain, M. Archary, Q. Bhorat, L. Fairlie, U. Lalloo, M. S. L. Masilela, D. Moodley, S. Hanley, L. Fouche, C. Louw, M. Tameris, N. Singh, A. Goga, K. Dheda, C. Grobbelaar, G. Kruger, N. Carrim-Ganey, V. Baillie, T. de Oliveira, A. L. Koen, J. J. Lombaard, R. Mngqibisa, A. E. Bhorat, G. Benadé, N. Lalloo, A. Pitsi, P.-L. Vollgraaff, A. Luabeya, A. Esmail, F. G. Petrick, A. Oommen-Jose, S. Foulkes, K. Ahmed, A. Thombrayil, L. Fries, S. Cloney-Clark, M. Zhu, C. Bennett, G. Albert, E. Faust, J. S. Plested, A. Robertson, S. Neal, I. Cho, G. M. Glenn, F. Dubovsky, S. A. Madhi, 2019nCoV-501 Study Group, Efficacy of NVX-CoV2373 Covid-19 Vaccine against the B.1.351 Variant, *New Engl J Med* **384**, 1899-1909 (2021).
19. L. J. Abu-Raddad, H. Chemaitelly, A. A. Butt, N. S. G. for C.-19 Vaccination, Effectiveness of the BNT162b2 Covid-19 Vaccine against the B.1.1.7 and B.1.351 Variants, *New Engl J Med* **385**, 187–189 (2021).
20. B. Agerer, M. Koblischke, V. Gudipati, L. F. Montaño-Gutierrez, M. Smyth, A. Popa, J.-W. Genger, L. Endler, D. M. Florian, V. Mühlgrabner, M. Graninger, S. W. Aberle, A.-M. Husa, L. E. Shaw, A. Lercher, P. Gattinger, R. Torralba-Gombau, D. Trapin, T. Penz, D. Barreca, I. Fae, S. Wenda, M. Traugott, G. Walder, W. F. Pickl, V. Thiel, F. Allerberger, H. Stockinger, E. Puchhammer-Stöckl, W. Weninger, G. Fischer, W. Hoepler, E. Pawelka, A. Zoufaly, R. Valenta, C. Bock, W. Paster, R. Geyeregger, M. Farlik, F. Halbritter, J. B. Huppa, J. H. Aberle, A. Bergthaler, SARS-CoV-2 mutations in MHC-I-restricted epitopes evade CD8+ T cell responses, *Sci Immunol* **6**, eabg6461 (2021).
21. T. I. de Silva, G. Liu, B. B. Lindsey, D. Dong, D. Shah, A. J. Mentzer, A. Angyal, R. Brown, M. D. Parker, Z. Ying, X. Yao, L. Turtle, S. Dunachie, C.-19 G. U. (COG-U. Consortium, M. K. Maini, G. Ogg, J. C. Knight, Y. Peng, S. L. Rowland-Jones, T. Dong, The impact of viral mutations on recognition by SARS-CoV-2 specific T-cells, *Biorxiv*, 2021.04.08.438904 (2021).

22. K. M. E. Gallagher, M. B. Leick, R. C. Larson, T. R. Berger, K. Katsis, J. Y. Yam, G. Brini, K. Grauwet, M. C.-19 C. & P. Team, M. V. Maus, SARS -CoV-2 T-cell immunity to variants of concern following vaccination, *Biorxiv,* 2021.05.03.442455 (2021).
23. C. Motozono, M. Toyoda, J. Zahradnik, A. Saito, H. Nasser, T. S. Tan, I. Ngare, I. Kimura, K. Uriu, Y. Kosugi, Y. Yue, R. Shimizu, J. Ito, S. Torii, A. Yonekawa, N. Shimono, Y. Nagasaki, R. Minami, T. Toya, N. Sekiya, T. Fukuhara, Y. Matsuura, G. Schreiber, G2P-J Consortium, T. Ikeda, S. Nakagawa, T. Ueno, K. Sato, SARS-CoV-2 spike L452R variant evades cellular immunity and increases infectivity, *Cell Host Microbe* **29**, 1124-1136.e11 (2021).
24. A. Tarke, J. Sidney, N. Methot, Y. Zhang, J. M. Dan, B. Goodwin, P. Rubiro, A. Sutherland, R. da S. Antunes, A. Frazier, S. A. Rawlings, D. M. Smith, B. Peters, R. H. Scheuermann, D. Weiskopf, S. Crotty, A. Grifoni, A. Sette, Impact of SARS-CoV-2 variants on the total $CD4^+$ and $CD8^+$ T cell reactivity in infected or vaccinated individuals, *Cell Rep Med* **2**, 100355 (2021).
25. A. Grifoni, D. Weiskopf, S. I. Ramirez, J. Mateus, J. M. Dan, C. R. Moderbacher, S. A. Rawlings, A. Sutherland, L. Premkumar, R. S. Jadi, D. Marrama, A. M. de Silva, A. Frazier, A. F. Carlin, J. A. Greenbaum, B. Peters, F. Krammer, D. M. Smith, S. Crotty, A. Sette, Targets of T Cell Responses to SARS-CoV-2 Coronavirus in Humans with COVID-19 Disease and Unexposed Individuals, *Cell* **181**, 1489-1501.e15 (2020).
26. J. M. Dan, J. Mateus, Y. Kato, K. M. Hastie, E. D. Yu, C. E. Faliti, A. Grifoni, S. I. Ramirez, S. Haupt, A. Frazier, C. Nakao, V. Rayaprolu, S. A. Rawlings, B. Peters, F. Krammer, V. Simon, E. O. Saphire, D. M. Smith, D. Weiskopf, A. Sette, S. Crotty, Immunological memory to SARS-CoV-2 assessed for up to 8 months after infection, *Science* **371**, eabf4063 (2021).
27. C. Riou, E. D. Bruyn, C. Stek, R. Daroowala, R. T. Goliath, F. Abrahams, Q. Said-Hartley, B. W. Allwood, N.-Y. Hsiao, K. A. Wilkinson, C. S. L. Arlehamn, A. Sette, S. Wasserman, R. J. Wilkinson, Relationship of SARS-CoV-2-specific CD4 response to COVID-19 severity and impact of HIV-1 and Tuberculosis co-infection, *J Clin Invest* **131**, e149125 (2021).
28. K. W. Cohen, S. L. Linderman, Z. Moodie, J. Czartoski, L. Lai, G. Mantus, C. Norwood, L. E. Nyhoff, V. V. Edara, K. Floyd, S. C. D. Rosa, H. Ahmed, R. Whaley, S. N. Patel, B. Prigmore, M. P. Lemos, C. W. Davis, S. Furth, J. O'Keefe, M. P. Gharpure, S. Gunisetty, K. A. Stephens, R. Antia, V. I. Zarnitsyna, D. S. Stephens, S. Edupuganti, N. Rouphael, E. J. Anderson, A. K. Mehta, J. Wrammert, M. S. Suthar, R. Ahmed, M. J. McElrath, Longitudinal analysis shows durable and broad immune memory after SARS-CoV-2 infection with persisting antibody responses and memory B and T cells, *Cell Rep Med* **2**, 100354 (2021).
29. D. M. Altmann, R. J. Boyton, R. Beale, Immunity to SARS-CoV-2 variants of concern, *Science* **371**, 1103–1104 (2021).
30. J. Mateus, A. Grifoni, A. Tarke, J. Sidney, S. I. Ramirez, J. M. Dan, Z. C. Burger, S. A. Rawlings, D. M. Smith, E. Phillips, S. Mallal, M. Lammers, P. Rubiro, L. Quiambao, A. Sutherland, E. D. Yu, R. da S. Antunes, J. Greenbaum, A. Frazier, A. J. Markmann, L. Premkumar, A. de Silva, B. Peters, S. Crotty, A. Sette, D. Weiskopf, Selective and cross-reactive SARS-CoV-2 T cell epitopes in unexposed humans, *Science* **370**, 89–94 (2020).
31. A. Tarke, J. Sidney, C. K. Kidd, J. M. Dan, S. I. Ramirez, E. D. Yu, J. Mateus, R. da S. Antunes, E. Moore, P. Rubiro, N. Methot, E. Phillips, S. Mallal, A. Frazier, S. A. Rawlings, J. A. Greenbaum, B. Peters, D. M. Smith, S. Crotty, D. Weiskopf, A. Grifoni, A. Sette, Comprehensive analysis of T cell immunodominance and immunoprevalence of SARS-CoV-2 epitopes in COVID-19 cases, *Cell Reports Medicine* **2**, 100204 (2021).

32. A. Nelde, T. Bilich, J. S. Heitmann, Y. Maringer, H. R. Salih, M. Roerden, M. Lübke, J. Bauer, J. Rieth, M. Wacker, A. Peter, S. Hörber, B. Traenkle, P. D. Kaiser, U. Rothbauer, M. Becker, D. Junker, G. Krause, M. Strengert, N. Schneiderhan-Marra, M. F. Templin, T. O. Joos, D. J. Kowalewski, V. Stos-Zweifel, M. Fehr, A. Rabsteyn, V. Mirakaj, J. Karbach, E. Jäger, M. Graf, L.-C. Gruber, D. Rachfalski, B. Preuß, I. Hagelstein, M. Märklin, T. Bakchoul, C. Gouttefangeas, O. Kohlbacher, R. Klein, S. Stevanović, H.-G. Rammensee, J. S. Walz, SARS-CoV-2-derived peptides define heterologous and COVID-19-induced T cell recognition, *Nat Immunol* **22**, 74–85 (2021).
33. V. Oberhardt, H. Luxenburger, J. Kemming, I. Schulien, K. Ciminski, S. Giese, B. Csernalabics, J. Lang-Meli, I. Janowska, J. Staniek, K. Wild, K. Basho, M. S. Marinescu, J. Fuchs, F. Topfstedt, A. Janda, O. Sogukpinar, H. Hilger, K. Stete, F. Emmerich, B. Bengsch, C. F. Waller, S. Rieg, Sagar, T. Boettler, K. Zoldan, G. Kochs, M. Schwemmle, M. Rizzi, R. Thimme, C. Neumann-Haefelin, M. Hofmann, Rapid and stable mobilization of CD8+ T cells by SARS-CoV-2 mRNA vaccine, *Nature* **597**, 268–273 (2021).
34. L. G. Thorne, M. Bouhaddou, A.-K. Reuschl, L. Zuliani-Alvarez, B. Polacco, A. Pelin, J. Batra, M. V. X. Whelan, M. Ummadi, A. Rojc, J. Turner, K. Obernier, H. Braberg, M. Soucheray, A. Richards, K.-H. Chen, B. Harjai, D. Memon, M. Hosmillo, J. Hiatt, A. Jahun, I. G. Goodfellow, J. M. Fabius, K. Shokat, N. Jura, K. Verba, M. Noursadeghi, P. Beltrao, D. L. Swaney, A. Garcia-Sastre, C. Jolly, G. J. Towers, N. J. Krogan, Evolution of enhanced innate immune evasion by the SARS-CoV-2 B.1.1.7 UK variant, *Biorxiv*, 2021.06.06.446826 (2021).
35. K. Guo, B. S. Barrett, K. L. Mickens, K. J. Hasenkrug, M. L. Santiago, Interferon Resistance of Emerging SARS-CoV-2 Variants, *Biorxiv*, 2021.03.20.436257 (2021).
36. C. J. Thieme, M. Anft, K. Paniskaki, A. Blazquez-Navarro, A. Doevelaar, F. S. Seibert, B. Hoelzer, M. J. Konik, M. M. Berger, T. Brenner, C. Tempfer, C. Watzl, T. L. Meister, S. Pfaender, E. Steinmann, S. Dolff, U. Dittmer, T. H. Westhoff, O. Witzke, U. Stervbo, T. Roch, N. Babel, Robust T Cell Response Toward Spike, Membrane, and Nucleocapsid SARS-CoV-2 Proteins Is Not Associated with Recovery in Critical COVID-19 Patients, *Cell Reports Medicine* **1**, 100092 (2020).
37. A. Abdel Latif, J. L. Mullen, M. Alkuzweny, G. Tsueng, M. Cano, E. Haag, J. Zhou, M. Zeller, E. Hufbauer, N. Matteson, C. Wu, K. G. Anderson, A. I. Su, K. Gangavarapu, L. D. Hughes, and the Center for Viral Systems Biology. S:L18F Mutation Report. Outbreak.info, (available at https://outbreak.onfo/situation-reports?pango&muts=S%3AL18F). Accessed 4 December 2021.
38. W. T. Harvey, A. M. Carabelli, B. Jackson, R. K. Gupta, E. C. Thomson, E. M. Harrison, C. Ludden, R. Reeve, A. Rambaut, S. J. Peacock, D. L. Robertson, SARS-CoV-2 variants, spike mutations and immune escape. *Nat Rev Microbiol* **19**, 1–16 (2021).
39. C. Scheepers, J. Everatt, D. G. Amoako, A. Mnguni, A. Ismail, B. Mahlangu, C. K. Wibmer, E. Wilkinson, H. Tegally, J. E. San, J. Giandhari, N. Ntuli, S. Pillay, T. Mohale, Y. Naidoo, Z. T. Khumalo, Z. Makatini, NGS-SA, A. Sigal, C. Williamson, F. Treurnicht, K. Mlisana, M. Venter, N. Hsiao, N. Wolter, N. Msomi, R. Lessells, T. Maponga, W. Preiser, P. L. Moore, A. von Gottberg, T. de Oliveira, J. N. Bhiman, The continuous evolution of SARS-CoV-2 in South Africa: a new lineage with rapid accumulation of mutations of concern and global detection, *Medrxiv*, 2021.08.20.21262342 (2021).
40. A. Abdel Latif, J. L. Mullen, M. Alkuzweny, G. Tsueng, M. Cano, E. Haag, J. Zhou, M. Zeller, E. Hufbauer, N. Matteson, C. Wu, K. G. Andersen, A. I. Su, K. Gangavarapu, L. D.

Hughes, and Center for Viral Systems Biology. outbreak.info, (available at https://outbreak.info/situation-reports), *Accessed 10 September 2021*.
41. T. Moyo-Gwete, M. Madzivhandila, Z. Makhado, F. Ayres, D. Mhlanga, B. Oosthuysen, B. E. Lambson, P. Kgagudi, H. Tegally, A. Iranzadeh, D. Doolabh, L. Tyers, L. R. Chinhoyi, M. Mennen, S. Skelem, G. Marais, C. K. Wibmer, J. N. Bhiman, V. Ueckermann, T. Rossouw, M. Boswell, T. de Oliveira, C. Williamson, W. A. Burgers, N. Ntusi, L. Morris, P. L. Moore, Cross-Reactive Neutralizing Antibody Responses Elicited by SARS-CoV-2 501Y.V2 (B.1.351), *New Engl J Med* **384**, 2161-2163 (2021).
42. M. Hoffmann, P. Arora, R. Groß, A. Seidel, B. F. Hörnich, A. S. Hahn, N. Krüger, L. Graichen, H. Hofmann-Winkler, A. Kempf, M. S. Winkler, S. Schulz, H.-M. Jäck, B. Jahrsdörfer, H. Schrezenmeier, M. Müller, A. Kleger, J. Münch, S. Pöhlmann, SARS-CoV-2 variants B.1.351 and P.1 escape from neutralizing antibodies, *Cell* **184**, 2384-2393.e12 (2021).
43. C. Liu, H. M. Ginn, W. Dejnirattisai, P. Supasa, B. Wang, A. Tuekprakhon, R. Nutalai, D. Zhou, A. J. Mentzer, Y. Zhao, H. M. E. Duyvesteyn, C. López-Camacho, J. Slon-Campos, T. S. Walter, D. Skelly, S. A. Johnson, T. G. Ritter, C. Mason, S. A. C. Clemens, F. G. Naveca, V. Nascimento, F. Nascimento, C. F. da Costa, P. C. Resende, A. Pauvolid-Correa, M. M. Siqueira, C. Dold, N. Temperton, T. Dong, A. J. Pollard, J. C. Knight, D. Crook, T. Lambe, E. Clutterbuck, S. Bibi, A. Flaxman, M. Bittaye, S. Belij-Rammerstorfer, S. C. Gilbert, T. Malik, M. W. Carroll, P. Klenerman, E. Barnes, S. J. Dunachie, V. Baillie, N. Serafin, Z. Ditse, K. D. Silva, N. G. Paterson, M. A. Williams, D. R. Hall, S. Madhi, M. C. Nunes, P. Goulder, E. E. Fry, J. Mongkolsapaya, J. Ren, D. I. Stuart, G. R. Screaton, Reduced neutralization of SARS-CoV-2 B.1.617 by vaccine and convalescent serum, *Cell* **184**, 4220-4236.e13 (2021).
44. D. Planas, D. Veyer, A. Baidaliuk, I. Staropoli, F. Guivel-Benhassine, M. M. Rajah, C. Planchais, F. Porrot, N. Robillard, J. Puech, M. Prot, F. Gallais, P. Gantner, A. Velay, J. L. Guen, N. Kassis-Chikhani, D. Edriss, L. Belec, A. Seve, L. Courtellemont, H. Péré, L. Hocqueloux, S. Fafi-Kremer, T. Prazuck, H. Mouquet, T. Bruel, E. Simon-Lorière, F. A. Rey, O. Schwartz, Reduced sensitivity of SARS-CoV-2 variant Delta to antibody neutralization, *Nature* **596**, 276–280 (2021).
45. D. Planas, D. Veyer, A. Baidaliuk, I. Staropoli, F. Guivel-Benhassine, M. M. Rajah, C. Planchais, F. Porrot, N. Robillard, J. Puech, M. Prot, F. Gallais, P. Gantner, A. Velay, J. L. Guen, N. Kassis-Chikhani, D. Edriss, L. Belec, A. Seve, L. Courtellemont, H. Péré, L. Hocqueloux, S. Fafi-Kremer, T. Prazuck, H. Mouquet, T. Bruel, E. Simon-Lorière, F. A. Rey, O. Schwartz, Reduced sensitivity of SARS-CoV-2 variant Delta to antibody neutralization. *Nature* **596**, 276–280 (2021).
46. L. Dupont, L. B. Snell, C. Graham, J. Seow, B. Merrick, T. Lechmere, T. J. A. Maguire, S. R. Hallett, S. Pickering, T. Charalampous, A. Alcolea-Medina, I. Huettner, J. M. Jimenez-Guardeño, S. Acors, N. Almeida, D. Cox, R. E. Dickenson, R. P. Galao, N. Kouphou, M. J. Lista, A. M. Ortega-Prieto, H. Wilson, H. Winstone, C. Fairhead, J. Z. Su, G. Nebbia, R. Batra, S. Neil, M. Shankar-Hari, J. D. Edgeworth, M. H. Malim, K. J. Doores, Neutralizing antibody activity in convalescent sera from infection in humans with SARS-CoV-2 and variants of concern. *Nat Microbiol* **6**, 1433–1442 (2021).
47. E. C. Wall, M. Wu, R. Harvey, G. Kelly, S. Warchal, C. Sawyer, R. Daniels, P. Hobson, E. Hatipoglu, Y. Ngai, S. Hussain, J. Nicod, R. Goldstone, K. Ambrose, S. Hindmarsh, R. Beale, A. Riddell, S. Gamblin, M. Howell, G. Kassiotis, V. Libri, B. Williams, C. Swanton, S.

Gandhi, D. L. Bauer, Neutralising antibody activity against SARS-CoV-2 VOCs B.1.617.2 and B.1.351 by BNT162b2 vaccination. *Lancet* **397**, 2331–2333 (2021).
48. S. Cele, L. Jackson, K. Khan, D. Khoury, T. Moyo-Gwete, H. Tegally, C. Scheepers, D. Amoako, F. Karim, M. Bernstein, G. Lustig, D. Archary, M. Smith, Y. Ganga, Z. Jule, K. Reedoy, J.Emmanuel San, S-H. Hwa, J. Giandhari, J. M. Blackburn, B. I. Gosnell, S. A. Karim, W. Hanekom, NGS-SA, COMMIT-KZN Team, A. von Gottberg, J. Bhiman, R. J. Lessells, M.-Y. S. Moosa, M. Davenport, T. de Oliveira, P. L. Moore, A. Sigal. SARS-CoV-2 Omicron has extensive but incomplete escape of Pfizer BNT162b2 elicited neutralization and requires ACE2 for infection. *MedRXiv* (2021).
49. D. S. Khoury, D. Cromer, A. Reynaldi, T. E. Schlub, A. K. Wheatley, J. A. Juno, K. Subbarao, S. J. Kent, J. A. Triccas, M. P. Davenport, Neutralizing antibody levels are highly predictive of immune protection from symptomatic SARS-CoV-2 infection, *Nat Med* **27**, 1205–1211 (2021).
50. K. A. Earle, D. M. Ambrosino, A. Fiore-Gartland, D. Goldblatt, P. B. Gilbert, G. R. Siber, P. Dull, S. A. Plotkin, Evidence for antibody as a protective correlate for COVID-19 vaccines, *Vaccine* **39**, 4423–4428 (2021).
51. K. McMahan, J. Yu, N. B. Mercado, C. Loos, L. H. Tostanoski, A. Chandrashekar, J. Liu, L. Peter, C. Atyeo, A. Zhu, E. A. Bondzie, G. Dagotto, M. S. Gebre, C. Jacob-Dolan, Z. Li, F. Nampanya, S. Patel, L. Pessaint, A. V. Ry, K. Blade, J. Yalley-Ogunro, M. Cabus, R. Brown, A. Cook, E. Teow, H. Andersen, M. G. Lewis, D. A. Lauffenburger, G. Alter, D. H. Barouch, Correlates of protection against SARS-CoV-2 in rhesus macaques, *Nature* **590**, 630–634 (2021).
52. C. R. Moderbacher, S. I. Ramirez, J. M. Dan, A. Grifoni, K. M. Hastie, D. Weiskopf, S. Belanger, R. K. Abbott, C. Kim, J. Choi, Y. Kato, E. G. Crotty, C. Kim, S. A. Rawlings, J. Mateus, L. P. V. Tse, A. Frazier, R. Baric, B. Peters, J. Greenbaum, E. O. Saphire, D. M. Smith, A. Sette, S. Crotty, Antigen-Specific Adaptive Immunity to SARS-CoV-2 in Acute COVID-19 and Associations with Age and Disease Severity, *Cell* **183**, 996-1012.e19 (2020).
53. S. K. Saini, D. S. Hersby, T. Tamhane, H. R. Povlsen, S. P. A. Hernandez, M. Nielsen, A. O. Gang, S. R. Hadrup, SARS-CoV-2 genome-wide T cell epitope mapping reveals immunodominance and substantial CD8+ T cell activation in COVID-19 patients, *Sci Immunol* **6**, eabf7550 (2021).
54. R. Parker, T. Partridge, C. Wormald, R. Kawahara, V. Stalls, M. Aggelakopoulou, J. Parker, R. P. Doherty, Y. A. Morejon, E. Lee, K. Saunders, B. F. Haynes, P. Acharya, M. Thaysen-Andersen, P. Borrow, N. Ternette, Mapping the SARS-CoV-2 spike glycoprotein-derived peptidome presented by HLA class II on dendritic cells, *Cell Reports* **35**, 109179 (2021).
55. Y. Peng, A. J. Mentzer, G. Liu, X. Yao, Z. Yin, D. Dong, W. Dejnirattisai, T. Rostron, P. Supasa, C. Liu, C. López-Camacho, J. Slon-Campos, Y. Zhao, D. I. Stuart, G. C. Paesen, J. M. Grimes, A. A. Antson, O. W. Bayfield, D. E. D. P. Hawkins, D.-S. Ker, B. Wang, L. Turtle, K. Subramaniam, P. Thomson, P. Zhang, C. Dold, J. Ratcliff, P. Simmonds, T. de Silva, P. Sopp, D. Wellington, U. Rajapaksa, Y.-L. Chen, M. Salio, G. Napolitani, W. Paes, P. Borrow, B. M. Kessler, J. W. Fry, N. F. Schwabe, M. G. Semple, J. K. Baillie, S. C. Moore, P. J. M. Openshaw, M. A. Ansari, S. Dunachie, E. Barnes, J. Frater, G. Kerr, P. Goulder, T. Lockett, R. Levin, Y. Zhang, R. Jing, L.-P. Ho, E. Barnes, D. Dong, T. Dong, S. Dunachie, J. Frater, P. Goulder, G. Kerr, P. Klenerman, G. Liu, A. McMichael, G. Napolitani, G. Ogg, Y. Peng, M. Salio, X. Yao, Z. Yin, J. K. Baillie, P. Klenerman, A. J. Mentzer, S. C. Moore, P. J. M. Openshaw, M. G. Semple, D. I. Stuart, L. Turtle, R. J. Cornall, C. P. Conlon, P.

Klenerman, G. R. Screaton, J. Mongkolsapaya, A. McMichael, J. C. Knight, G. Ogg, T. Dong, Broad and strong memory CD4+ and CD8+ T cells induced by SARS-CoV-2 in UK convalescent individuals following COVID-19, *Nat Immunol* **21**, 1336–1345 (2020).
56. J. A. Juno, D. van Bockel, S. J. Kent, A. D. Kelleher, J. J. Zaunders, C. M. L. Munier, Cytotoxic CD4 T Cells—Friend or Foe during Viral Infection?, *Front Immunol* **8**, 19 (2017).
57. B. J. Meckiff, C. Ramírez-Suástegui, V. Fajardo, S. J. Chee, A. Kusnadi, H. Simon, S. Eschweiler, A. Grifoni, E. Pelosi, D. Weiskopf, A. Sette, F. Ay, G. Seumois, C. H. Ottensmeier, P. Vijayanand, Imbalance of Regulatory and Cytotoxic SARS-CoV-2-Reactive CD4+ T Cells in COVID-19, *Cell* **183**, 1340-1353.e16 (2020).
58. N. Kaneko, J. Boucau, H.-H. Kuo, C. Perugino, V. S. Mahajan, J. R. Farmer, H. Liu, T. J. Diefenbach, A. Piechocka-Trocha, K. Lefteri, M. T. Waring, K. R. Premo, B. D. Walker, J. Z. Li, G. Gaiha, X. G. Yu, M. Lichterfeld, R. F. Padera, S. Pillai, Expansion of Cytotoxic CD4+ T cells in the lungs in severe COVID-19, *Medrxiv*, 2021.03.23.21253885 (2021).
59. A. Fiore-Gartland, B. A. Manso, D. P. Friedrich, E. E. Gabriel, G. Finak, Z. Moodie, T. Hertz, S. C. D. Rosa, N. Frahm, P. B. Gilbert, M. J. McElrath, Pooled-Peptide Epitope Mapping Strategies Are Efficient and Highly Sensitive: An Evaluation of Methods for Identifying Human T Cell Epitope Specificities in Large-Scale HIV Vaccine Efficacy Trials, *Plos One* **11**, e0147812 (2016).
60. R. Keeton, S. I. Richardson, T. Moyo-Gwete, T. Hermanus, M. B. Tincho, N. Benede, N. P. Manamela, R, Baguma, Z. Makhado, A. Ngomti, T. Motlou, M. Mennen, L. Chinhoyi, S. Skelem, H. Maboreke, D. Doolabh, A. Iranzadeh, A. D. Otter, T. Brooks, M. Noursadeghi, J. Moon, J. Blackburn, N-Y. Hsiao, C. Williamson, C. Riou, A. Goga, N. Garrett, L-G. Bekker, G. Gray, N. A. B. Ntusi, P. L. Moore, W. A. Burgers, Prior infection with SARS-CoV-2 boosts and broadens Ad26.COV2.S immunogenicity in a variant dependent manner, *Medrxiv*, 2021.07.24.21261037 (2021).
61. A. Tarke, J. Sidney, N. Methot, E. D. Yu, Y. Zhang, J. M. Dan, B. Goodwin, P. Rubiro, A. Sutherland, E. Wang, A. Frazier, S. I. Ramirez, S. A. Rawlings, D. M. Smith, R. da S. Antunes, B. Peters, R. H. Scheuermann, D. Weiskopf, S. Crotty, A. Grifoni, A. Sette, Impact of SARS-CoV-2 variants on the total CD4+ and CD8+ T cell reactivity in infected or vaccinated individuals. *Cell Reports Medicine* **2**, 100355 (2021).
62. D. Geers, M. C. Shamier, S. Bogers, G. den Hartog, L. Gommers, N. N. Nieuwkoop, K. S. Schmitz, L. C. Rijsbergen, J. A. T. van Osch, E. Dijkhuizen, G. Smits, A. Comvalius, D. van Mourik, T. G. Caniels, M. J. van Gils, R. W. Sanders, B. B. O. Munnink, R. Molenkamp, H. J. de Jager, B. L. Haagmans, R. L. de Swart, M. P. G. Koopmans, R. S. van Binnendijk, R. D. de Vries, C. H. GeurtsvanKessel, SARS-CoV-2 variants of concern partially escape humoral but not T-cell responses in COVID-19 convalescent donors and vaccinees, *Sci Immunol* **6**, eabj1750 (2021).
63. C. J. Reynolds, C. Pade, J. M. Gibbons, D. K. Butler, A. D. Otter, K. Menacho, M. Fontana, A. Smit, J. E. Sackville-West, T. Cutino-Moguel, M. K. Maini, B. Chain, M. Noursadeghi, U. Covid. I. C. Network, T. Brooks, A. Semper, C. Manisty, T. A. Treibel, J. C. Moon, U. Covid. Investigators, A. M. Valdes, Á. McKnight, D. M. Altmann, R. Boyton, Prior SARS-CoV-2 infection rescues B and T cell responses to variants after first vaccine dose, *Science*, eabh1282 (2021).
64. S. Cleemput, W. Dumon, V. Fonseca, W. A. Karim, M. Giovanetti, L. C. Alcantara, K. Deforche, T. de Oliveira, Genome Detective Coronavirus Typing Tool for rapid identification and characterization of novel coronavirus genomes, *Bioinformatics* **36**, 3552–3555 (2020).

65. J. Hadfield, C. Megill, S. M. Bell, J. Huddleston, B. Potter, C. Callender, P. Sagulenko, T. Bedford, R. A. Neher, Nextstrain: real-time tracking of pathogen evolution, *Bioinformatics* **34**, 4121–4123 (2018).
66. G. Yu, D. K. Smith, H. Zhu, Y. Guan, T. T. Lam, ggtree: an r package for visualization and annotation of phylogenetic trees with their covariates and other associated data, *Methods Ecol Evol* **8**, 28–36 (2017).
67. S. Paul, J. Sidney, A. Sette, B. Peters, TepiTool: A Pipeline for Computational Prediction of T Cell Epitope Candidates, *Curr Protoc Immunol* **114**, 18.19.1-18.19.24 (2016).
68. K. K. Jensen, M. Andreatta, P. Marcatili, S. Buus, J. A. Greenbaum, Z. Yan, A. Sette, B. Peters, M. Nielsen, Improved methods for predicting peptide binding affinity to MHC class II molecules, *Immunology* **154**, 394–406 (2018).
69. M. Andreatta, E. Karosiene, M. Rasmussen, A. Stryhn, S. Buus, M. Nielsen, Accurate pan-specific prediction of peptide-MHC class II binding affinity with improved binding core identification, *Immunogenetics* **67**, 641–650 (2015).
70. J. Sidney, E. Assarsson, C. Moore, S. Ngo, C. Pinilla, A. Sette, B. Peters, Quantitative peptide binding motifs for 19 human and mouse MHC class I molecules derived using positional scanning combinatorial peptide libraries, *Immunome Res* **4**, 2 (2008).
71. M. Nielsen, C. Lundegaard, O. Lund, Prediction of MHC class II binding affinity using SMM-align, a novel stabilization matrix alignment method, *Bmc Bioinformatics* **8**, 238 (2007).
72. T. Sturniolo, E. Bono, J. Ding, L. Raddrizzani, O. Tuereci, U. Sahin, M. Braxenthaler, F. Gallazzi, M. P. Protti, F. Sinigaglia, J. Hammer, Generation of tissue-specific and promiscuous HLA ligand databases using DNA microarrays and virtual HLA class II matrices, *Nat Biotechnol* **17**, 555–561 (1999).

Acknowledgments: We thank the study participants and their families, and the clinical staff and personnel at Groote Schuur Hospital for their support and dedication. We thank the informal Variant consortium of South Africa, chaired by Drs Willem Hanekom and Tulio de Oliveira, for suggestions and discussion of data. For the purposes of open access, the authors have applied a CC BY public copyright license to any author-accepted version arising from this submission.

Funding: This research was supported by the South African Medical Research Council, with funds received from the South African Department of Science and Innovation (DSI), and the Wellcome Centre for Infectious Diseases Research in Africa (CIDRI-Africa), which is supported by core funding from the Wellcome Trust [203135/Z/16/Z]. CR and WAB are supported by the EDCTP2 programme of the European Union (EU)'s Horizon 2020 programme (TMA2017SF-1951-TB-SPEC to CR and TMA2016SF-1535-CaTCH-22 to WAB). This work is further

supported by the National Institutes of Health (R21AI148027 to CR), Francis Crick Institute, which receives funding from Wellcome FC0010218, UKRI FC0010218 and CRUK FC0010218 and the Rosetrees Trust grant M926 (to CR and RJW). PLM is supported by the South African Research Chairs Initiative of the DSI and the National Research Foundation (Grant No 9834). NABN acknowledges funding from the SA-MRC, MRC UK, NRF, and the Lily and Ernst Hausmann Trust.

Author contributions: WAB, CR, PLM, NABN and RJW conceived and designed the study, acquired funding and supervised the work. LRC, MM, SS, EdB and CS recruited the study participants. CR, RK, RB, HM, MBT and NB performed the T cell experiments. TH, TM-G and PK performed the neutralizing assays. ZV-O and MS performed HLA typing. HT, DD, LT, AI, GM, CW and TdO performed the sequencing and phylogenetic analyses. CR and WAB analyzed the data and wrote the manuscript, with all authors contributing by providing critical feedback and final review.

Competing interests: The authors declare that they have no competing interests.

Data and materials availability: All data are available in the main text or the supplementary materials.

Figure Legends

Fig. 1. T cell recognition of SARS-CoV-2 spike in first and second wave COVID-19 patients. (**A**) Clinical characteristics of acute COVID-19 patients recruited during the first and second wave of the COVID-19 pandemic in South Africa. *: median and interquartile range. $^{\$}$: Disease severity was defined based on oxygen therapy requirement according to the WHO ordinal scale scoring system; Moderate (no O_2 or O_2 via nasal prongs) or severe (O_2 via high flow to ECMO).

[#]: SARS-CoV-2 polymerase chain reaction (PCR) was performed using the Allplex™ 2019-nCoV Assay (Seegene). The cycle threshold (CT) value for the N-gene is reported. (**B**) SARS-CoV-2 epidemiological dynamics in the Western Cape (South Africa). Prevalence of SARS-CoV-2 strains is on the left y-axis (based on sequencing 4549 samples). Ancestral strains are depicted in blue, Beta in red, Alpha in grey and Delta in green. Monthly COVID-19 cases are on the right y-axis. Bars above the graph indicate when samples were collected. (**C**) Representative flow cytometry plots of IFN-γ, TNF-α and IL-2 production by CD4 T cells in response to ancestral full spike peptide pool (Full Spike) in one first wave (blue) and one second wave (red) COVID-19 patient. Frequencies of cytokine-producing cells are indicated. (**D**) Frequency of SARS-CoV-2-specific CD4 or CD8 T cells producing IFN-γ, TNF-α or IL-2, in first wave (n = 22, blue) and second wave (n = 22, red) COVID-19 patients. Bars represent medians of responders. Statistical analyses were performed using the Mann-Whitney test between T cell responders from the first and second wave and the Wilcoxon test between CD4 and CD8 responders. **(E)** Comparison of polyfunctional profiles of SARS-CoV-2-specific CD4 T cells in first and second wave patients. **(F)** Comparison of polyfunctional profiles of SARS-CoV-2-specific CD8 T cells in first and second wave patients. The medians are shown. Each response pattern is color-coded, and data summarized in the pie charts. Statistical differences between pies were defined using a permutation test.

Fig. 2. T cell recognition of WT SARS-CoV-2 spike (S), nucleocapsid (N) and membrane (M) proteins in first and second wave convalescent COVID-19 patients. (A) Clinical characteristics of convalescent COVID-19 patients recruited during the first and second wave of the COVID-19 pandemic. *: median and interquartile range. [$]: Disease severity was defined based on oxygen therapy requirement according to the WHO ordinal scale scoring system. **(B)** Summary graph of the frequency of ancestral SARS-CoV-2 S-, N- or M-specific CD4 or CD8 T cells, producing IFN-γ, TNF-α or IL-2, in first wave (n = 10, light blue) and second wave (n = 14, orange) convalescent COVID-19 patients. Due to limited cell availability, T cell responses to M were tested in 10 first wave participants and 7 second wave participants. The proportion of participants exhibiting a detectable CD8 response is indicated. Bars represent medians of responders. Statistical analyses were performed using the Mann-Whitney test. **(C&D)**

Polyfunctional profiles of ancestral Spike-specific CD4 and CD8 T cells in first and second wave convalescent COVID-19 patients. Medians and IQR are shown. Each response pattern is color-coded, and data is summarized in pie charts. Statistical differences between pies were defined using a permutation test.

Fig. 3. Loss of recognition of SARS-CoV-2 Beta variant epitopes and neutralizing antibody responses. (**A**) Representative flow cytometry plots of IFN-γ production by CD4 T cells in response to ancestral full spike peptide pool (Full spike), and smaller pools spanning the mutated regions of ancestral (WT pool) or Beta spike (Beta pool) in two first wave (blue) and two second wave (red) COVID-19 patients. Frequencies (%) of IFN-γ positive cells are indicated. (**B**) The frequency of IFN-γ-producing SARS-CoV-2-specific CD4 T cells in first wave (n = 22, left) and second wave (n = 22, right) COVID-19 patients. The proportion of patients exhibiting a detectable response to the different peptide pools (i.e., responders) is indicated at the bottom of each graph. (**C**) Plasma samples from COVID-19 patients recruited during the first (n = 18) or the second wave (n = 19) were tested for neutralization cross-reactivity against ancestral or Beta pseudoviruses. The threshold of detection was a 50% inhibitory dilution (ID_{50}) of 20. Gray dots indicate patients who displayed a detectable CD4 T cell response to WT pool, selectively covering the variable regions of spike, and lost recognition to the Beta pool. Neutralization data on the second wave cohort are from *(25).* (**D**) Fold-change in neutralization titers is shown for data in **c**. Bars represent medians. Statistical analyses were performed using the Wilcoxon test and the Fisher's exact-squared test.

Fig. 4. Infrequent recognition of SARS-CoV-2 ancestral or Beta variant spike epitopes by CD8 T cells. (**A**) Representative flow cytometry plots of IFN-γ production by CD8 T cells in response to ancestral full spike peptide pool (Full Spike), and pools covering the mutated regions of ancestral spike (WT pool) or Beta spike (Beta pool) in two first wave (blue) and two second wave (red) COVID-19 patients. Frequencies (%) of IFN-γ positive cells are indicated. (**B**) Frequency of IFN-γ-producing SARS-CoV-2-specific CD8 T cells in first wave (n = 22, left) and second wave (n = 22, right) patients. The proportion of responders is indicated. Bars represent medians. Statistical analyses were performed using the Wilcoxon test.

Fig. 5: Identification of SARS-CoV-2 spike epitopes targeted by CD4 T cells. (A) Representative flow plots of IFN-γ production by CD8 and CD4 T cells in response to the Beta pool, WT pool and peptide pairs containing the spike 6-25 sequence (containing L18), the 73-92 sequence (containing D80) and the 206-225 sequence (containing D215) in three first wave patients. HLA Class-II alleles of each participant are listed on the right. **(B)** Number of tested first wave participants (n = 6) exhibiting a response to Beta pool, WT pool and each of the peptide pairs tested individually. **(C)** Frequency of IFN-γ+ CD4 T cells in response to indicated stimuli. Each participant is depicted by a different color.

Figure 1

A

	Hospitalized COVID-19 patients		
	1st wave	2nd wave	*P* value
N	22	22	
Sampling date	11 Jun - 21 Aug	31 Dec - 15 Jan	
Age*	53 [40-57]	55 [45-60]	0.49
Gender (% female)	45.5 %	68.2 %	0.13
Days post symptoms*	10 [8-10]	not known	
Days post PCR+*	4.5 [3-7]	8 [5-12]	0.006
CT values #,*	32.7 [29.9-35.8]	33 [29.6-35.8]	0.88
Moderate disease (%)$	50%	81.8%	0.054
Severe disease (%)$	50%	18.2%	
Viral sequence	Not available	Available (n=19)	

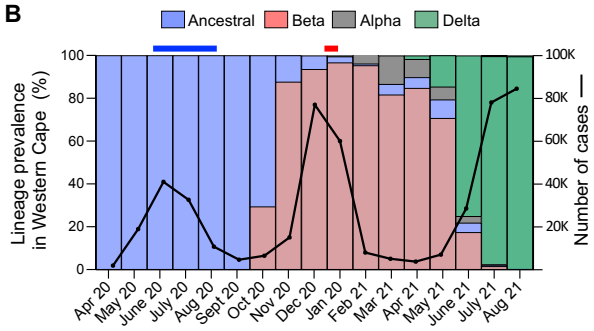

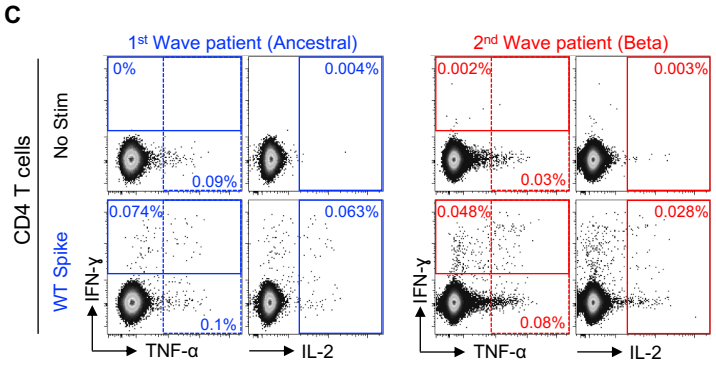

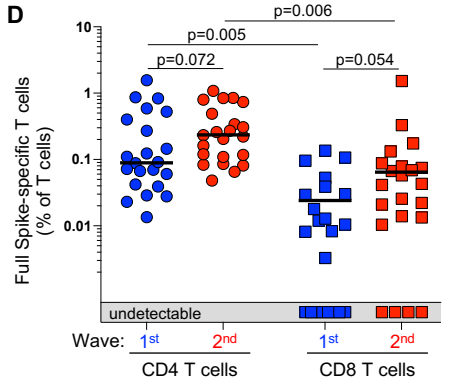

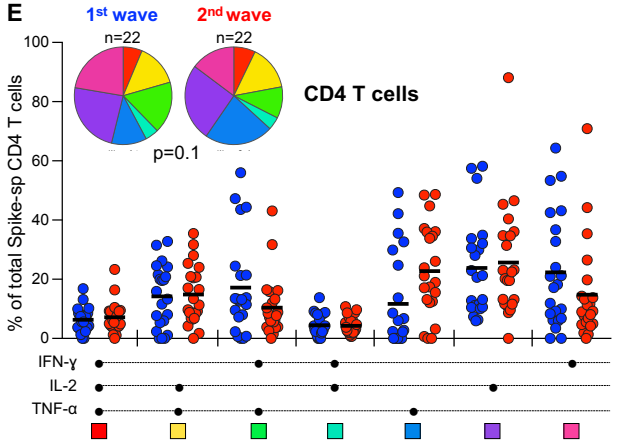

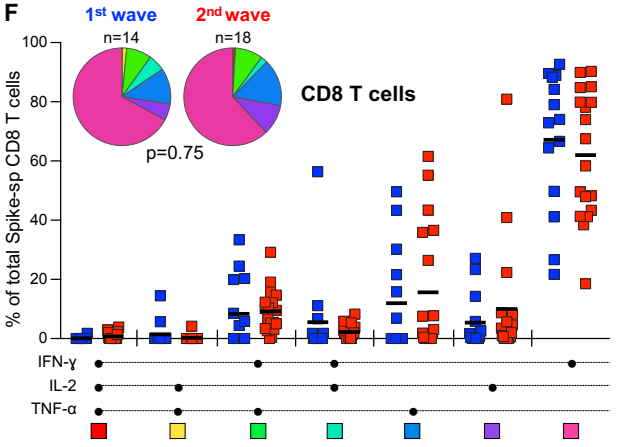

A

	Convalescent COVID-19 patients		
	1st wave	2nd wave	*P* value
N	10	14	
Date PCR+ test	01 Jul - 28 Sept	06 Nov - 29 Dec	
Age*	39 [34-47]	34 [31-42]	0.29
Gender (% female)	70%	78.6%	0.63
Days post PCR+*	83 [72-103]	73 [55-94]	0.28
Mild disease (%)$	100%	100%	

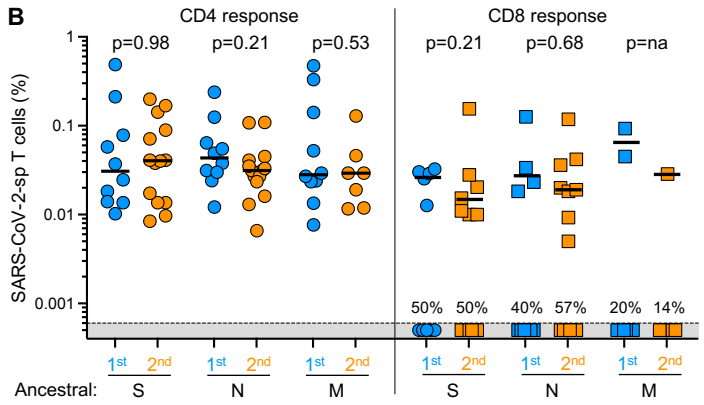

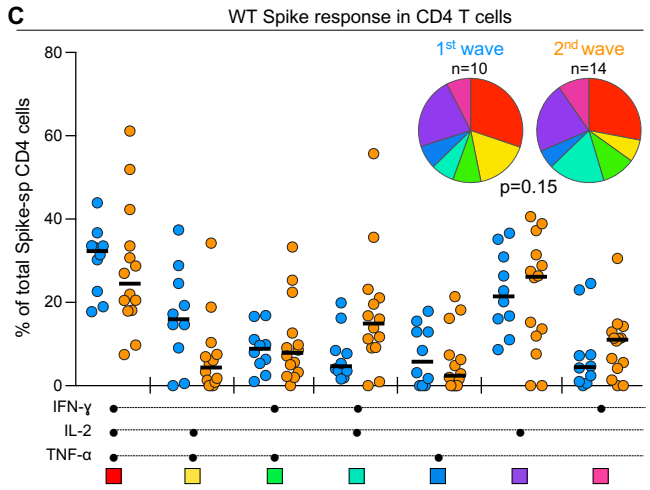

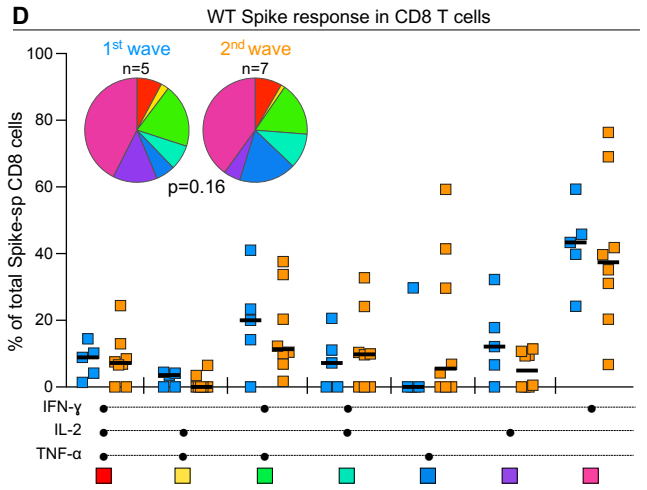

Figure 3

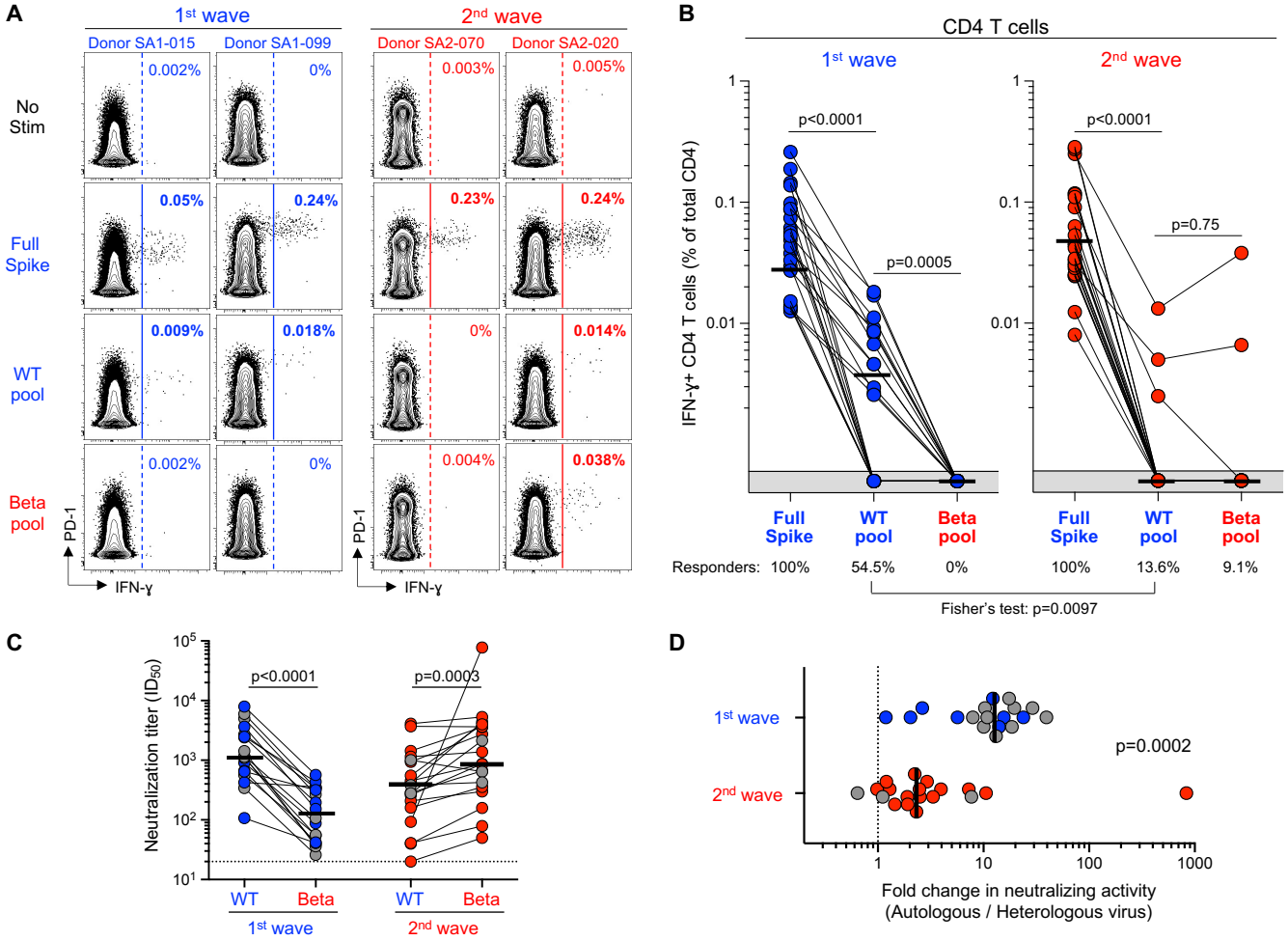
A
1st wave
2nd wave
Donor SA1-015
Donor SA1-099
Donor SA2-070
Donor SA2-020
No Stim
Full Spike
WT pool
Beta pool
0.002%
0%
0.003%
0.005%
0.05%
0.24%
0.23%
0.24%
0.009%
0.018%
0%
0.014%
0.002%
0%
0.004%
0.038%
PD-1
IFN-γ
B
CD4 T cells
1st wave
2nd wave
IFN-γ+ CD4 T cells (% of total CD4)
p<0.0001
p=0.0005
p<0.0001
p=0.75
Full Spike
WT pool
Beta pool
Responders: 100% 54.5% 0% 100% 13.6% 9.1%
Fisher's test: p=0.0097
C
Neutralization titer (ID50)
p<0.0001
p=0.0003
WT
Beta
1st wave
2nd wave
D
1st wave
2nd wave
p=0.0002
Fold change in neutralizing activity
(Autologous / Heterologous virus)

Figure 4

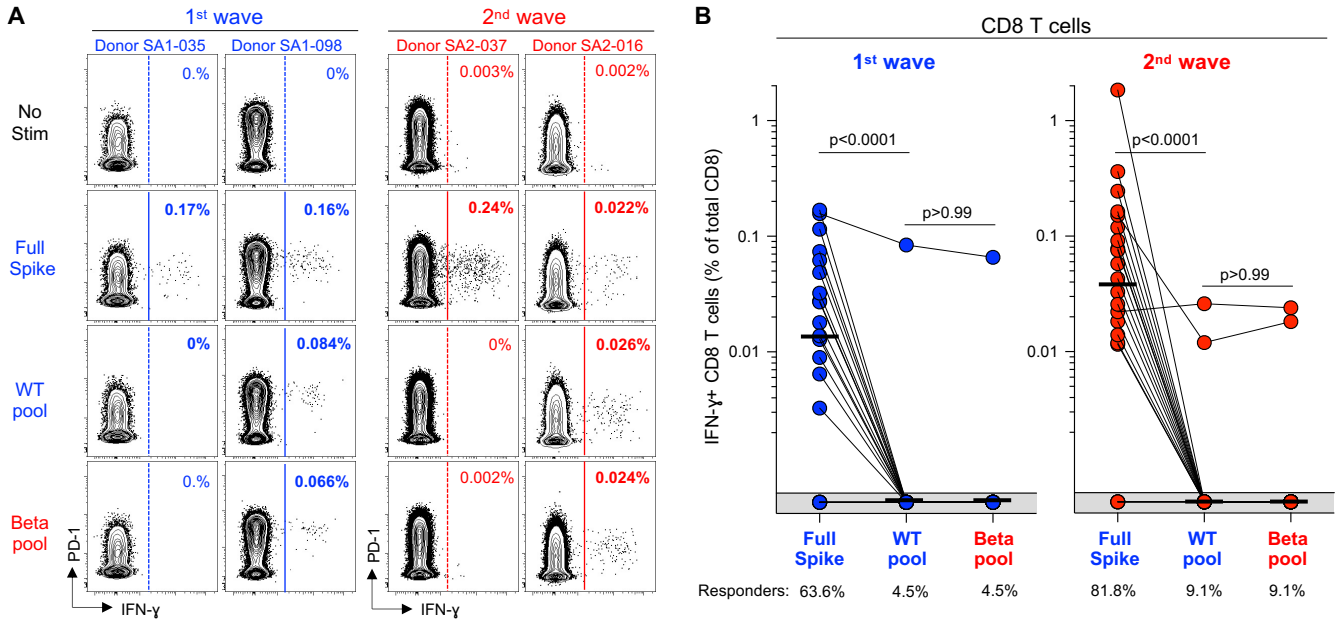
A
1st wave
2nd wave
Donor SA1-035
Donor SA1-098
Donor SA2-037
Donor SA2-016
No Stim
Full Spike
WT pool
Beta pool
0.%
0%
0.003%
0.002%
0.17%
0.16%
0.24%
0.022%
0%
0.084%
0%
0.026%
0.%
0.066%
0.002%
0.024%
PD-1
IFN-γ
B
CD8 T cells
1st wave
2nd wave
IFN-γ+ CD8 T cells (% of total CD8)
p<0.0001
p>0.99
Full Spike
WT pool
Beta pool
Responders:
63.6%
4.5%
4.5%
81.8%
9.1%
9.1%

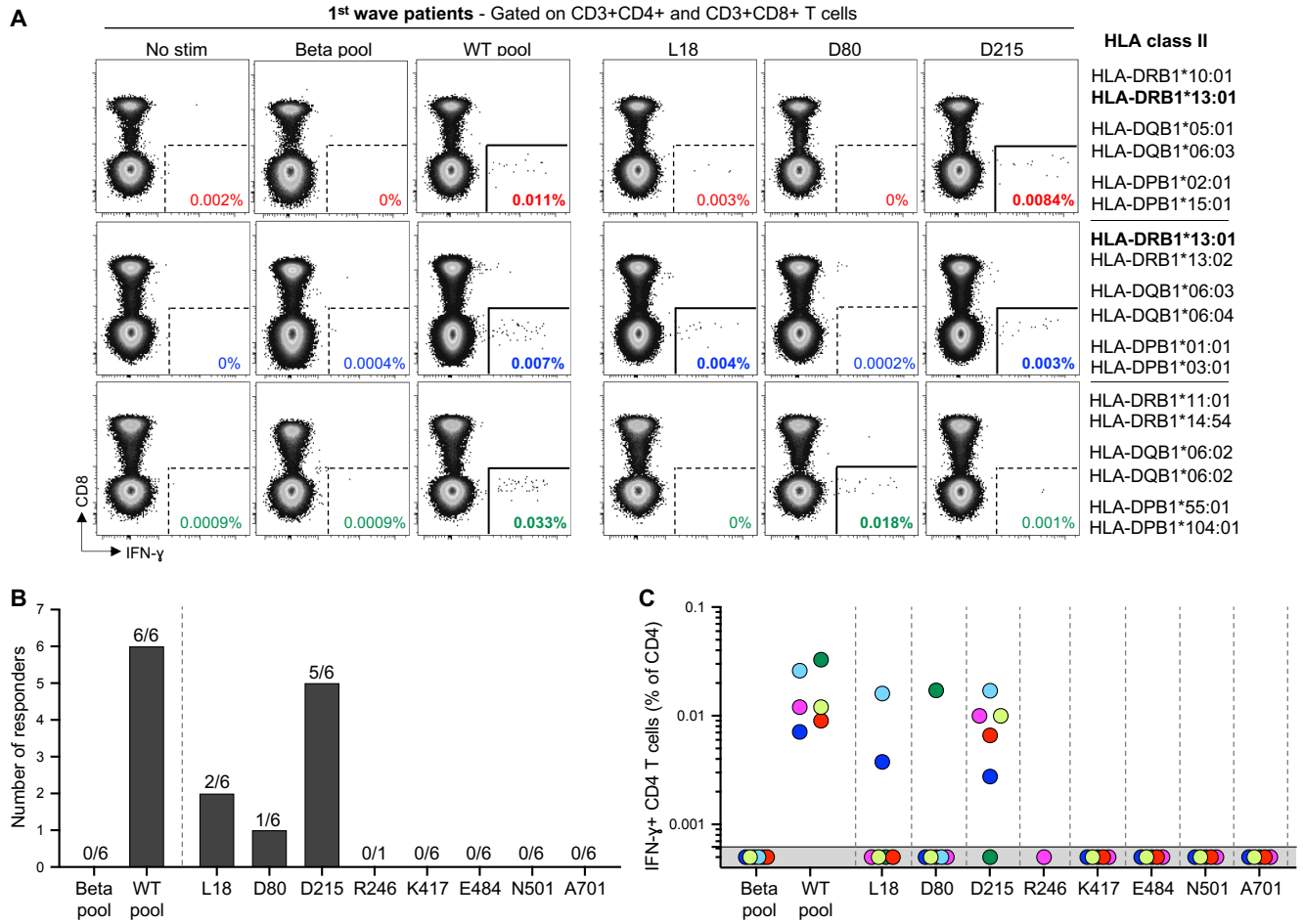
A
1st wave patients - Gated on CD3+CD4+ and CD3+CD8+ T cells
No stim
Beta pool
WT pool
L18
D80
D215
HLA class II
HLA-DRB1*10:01
HLA-DRB1*13:01
HLA-DQB1*05:01
HLA-DQB1*06:03
HLA-DPB1*02:01
HLA-DPB1*15:01
HLA-DRB1*13:01
HLA-DRB1*13:02
HLA-DQB1*06:03
HLA-DQB1*06:04
HLA-DPB1*01:01
HLA-DPB1*03:01
HLA-DRB1*11:01
HLA-DRB1*14:54
HLA-DQB1*06:02
HLA-DQB1*06:02
HLA-DPB1*55:01
HLA-DPB1*104:01
0.002%
0%
0.011%
0.003%
0%
0.0084%
0%
0.0004%
0.007%
0.004%
0.0002%
0.003%
0.0009%
0.0009%
0.033%
0%
0.018%
0.001%
CD8
IFN-γ
B
Number of responders
6/6
5/6
2/6
1/6
0/6
0/1
0/6
0/6
0/6
0/6
Beta pool
WT pool
L18
D80
D215
R246
K417
E484
N501
A701
C
IFN-γ+ CD4 T cells (% of CD4)
0.1
0.01
0.001

SUPPLEMENTARY MATERIALS

Loss of recognition of SARS-CoV-2 Beta variant spike epitopes but overall preservation of T cell immunity

Catherine Riou*, Roanne Keeton, Thandeka Moyo-Gwete, Tandile Hermanus, Prudence Kgagudi, Richard Baguma, Ziyaad Valley-Omar, Mikhail Smith, Houriiyah Tegally, Deelan Doolabh, Arash Iranzadeh, Lynn Tyers, Hygon Mutavhatsindi, Marius B. Tincho, Ntombi Benede, Gert Marais, Lionel R. Chinhoyi, Mathilda Mennen, Sango Skelem, Elsa du Bruyn, Cari Stek, SA-CIN, Tulio de Oliveira, Carolyn Williamson, Penny L. Moore, Robert J. Wilkinson, Ntobeko A. B. Ntusi, Wendy A. Burgers*

*Corresponding authors. Catherine Riou (cr.riou@uct.ac.za) and Wendy Burgers (wendy.burgers@uct.ac.za)

The PDF file includes:

Supplementary figures

- **Fig. S1**. Genomic sequencing confirmation of SARS-CoV-2 Beta infection of COVID-19 second wave patients.
- **Fig. S2.** Comparison of the frequency and polyfunctionality of T cell response to ancestral SARS-CoV-2 spike protein between acute and convalescent COVID-19 patients.
- **Fig. S3**. Relationship between SARS-CoV-2-specific CD4 T cell response and neutralizing activity in acute COVID-19 patients.
- **Fig. S4**. Graphical representation of study approach.
- **Fig. S5**. Flow cytometry gating strategy.

Supplementary tables

- **Table S1.** Peptides included in the ancestral and Beta peptide pools.
- **Table S2**. List of CD4+ T cell epitopes used in this study and their predicted HLA class II restriction(s).
- **Table S3**. HLA class II genotype (DRB1, DQB1 and DPB1) of COVID-19 patients.
- **Table S4.** List of spike epitopes tested and their predicted HLA Class II restriction.
- **Table S5.** HLA class I genotype (HLA-A, -B and -C) of COVID-19 patients.

Other Supplementary Material for this manuscript includes the following:

- **Data file S1** (Microsoft Excel format). HLA class II binding prediction for the 16 peptides included in the WT or Beta pool for HLA-DRB1, HLA-DQB1 and HLA-DPB1 alleles identified in the study cohort.
- **Data file S2** (Microsoft Excel format). Prevalence of HLA-DRB1, HLA-A and HLA-B in patients recruited during 1st and 2nd wave of the COVID-19 epidemic.
- **Data file S3** (Microsoft Excel format). HLA class I binding prediction for the 16 peptides included in the WT or Beta pool for HLA-A and HLA-B alleles identified in the study cohort.
- **Data file S4** (Microsoft Excel format). Raw data for each Figure and Supplementary Figure.

Supplementary Figure S1

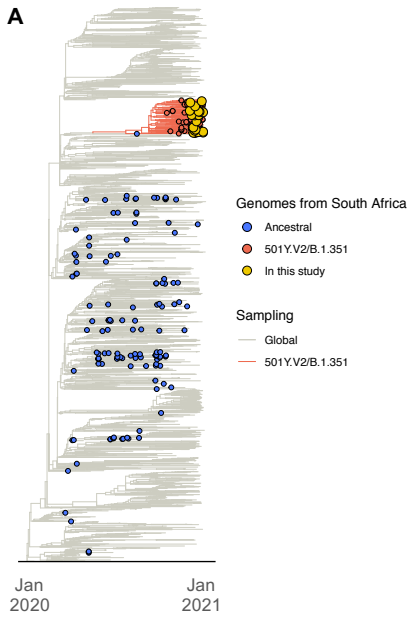

B

	Position & amino acid								
	18	80	215	242-244	246	417	484	501	701
Ancestral	L	D	D	LAL	R	K	E	N	A
Beta	F	A	G	- - -	I	N	K	Y	V
SA2-002	F	A	G	- - -	R	N	K	Y	V
SA2-006	L	A	G	- - -	R	N	K	Y	V
SA2-011	L	A	G	- - -	R	N	K	Y	V
SA2-012	L	A	G	- - -	R	N	K	Y	V
SA2-013	L	A	G	- - -	R	N	K	Y	V
SA2-017	L	A	G	- - -	R	N	K	Y	V
SA2-020**	L	A	G	- - -	R	N	K	Y	V
SA2-024	L	A	G	- - -	R	N	K	Y	V
SA2-029**	L	A	D	- - -	I	N	K	Y	V
SA2-037	L	A	G	- - -	R	N	K	Y	V
SA2-042	F	A	G	- - -	R	N	K	Y	V
SA2-043	F	A	G	- - -	R	N	K	Y	V
SA2-056	F	A	G	- - -	R	N	K	Y	V
SA2-070	F	A	G	- - -	R	N	K	Y	V
SA2-084	F	A	G	- - -	R	N	K	Y	V
SA2-094*	L	A	G	- - -	R	N	K	Y	V
SA2-095	F	A	G	- - -	R	N	K	Y	V
SA2-100	F	A	G	- - -	R	N	K	Y	V
SA2-102	F	A	G	- - -	R	N	K	Y	V
SA2-003	No sequence available								
SA2-016	No sequence available								
SA2-052	No sequence available								

Fig. S1. Genomic sequencing confirmation of SARS-CoV-2 Beta infection of COVID-19 second wave patients. (A) A time-resolved maximum clade credibility phylogeny of 2621 global SARS-CoV-2 sequences. Sequences from South Africa (n=209) are denoted with tip points. The Beta cluster is highlighted in red, and the genomes from this study (n=19) are shown in yellow, all falling in that cluster. **(B)** Spike sequence in patients recruited during the second wave, indicating amino acid changes. Blue shading corresponds with the ancestral strain (i.e., wild type, WT) amino acids and red shading to Beta variant amino acids. (-) corresponds to amino acid deletions. **: Patients exhibiting a detectable CD4 T cell response to the WT and Beta peptide pools, *: Patient exhibiting a detectable CD4 T cell response to the WT peptide pool.

Supplementary Figure S2

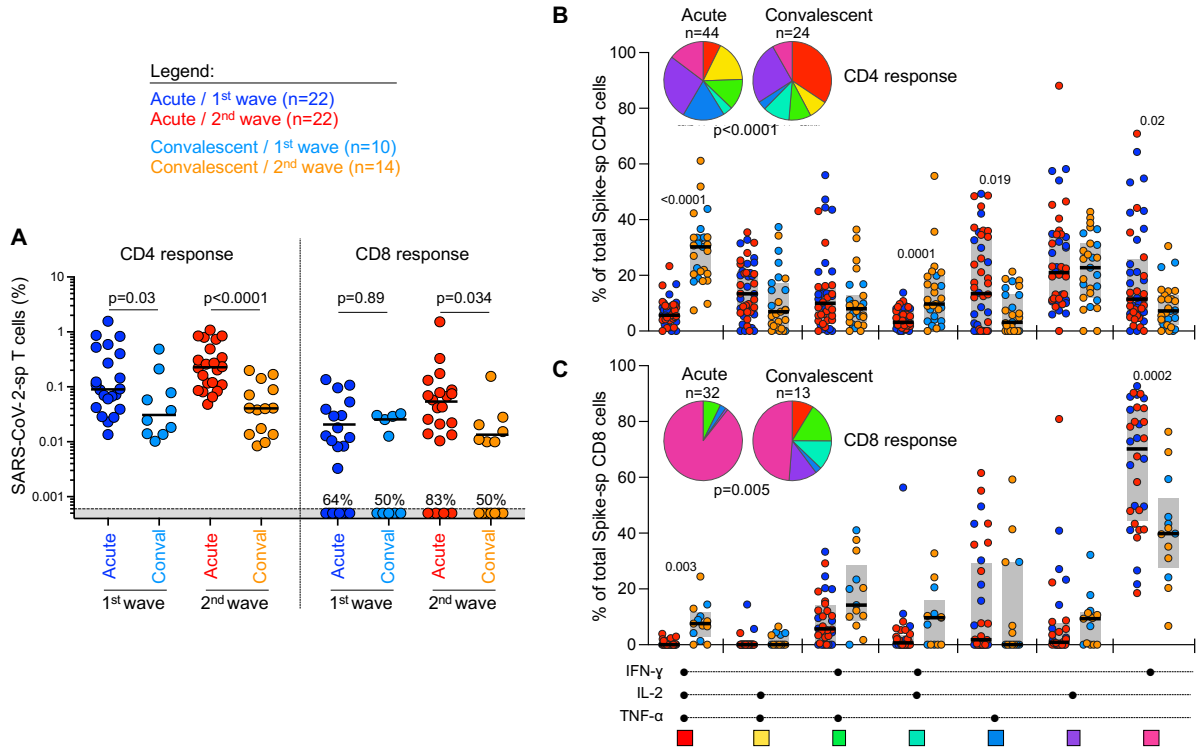

Fig. S2. Comparison of the frequency and polyfunctionality of T cell responses to ancestral SARS-CoV-2 Spike protein between acute and convalescent COVID-19 patients. (A) Summary graph of the frequency of ancestral SARS-CoV-2 Spike-specific CD4 and CD8 T cells, producing IFN-γ, TNF-α or IL-2, in acute and convalescent (~3 months post positive PCR) COVID-19 patients recruited during the first wave or second COVID-19 wave. The proportion of participant exhibiting a detectable CD8 response is indicated on the graph. Bars represent medians of responders. Statistical analyses were performed using the Mann-Whitney test including only participants with a detectable response. **(B&C)** Polyfunctional profile of ancestral Spike-specific CD4 (top) and CD8 (bottom) T cells in acute and convalescent COVID-19 patients. The medians and IQR are shown. Each response pattern is color-coded, and data are summarized in the pie charts. Statistical differences between pies were defined using a permutation test.

Supplementary Figure S3

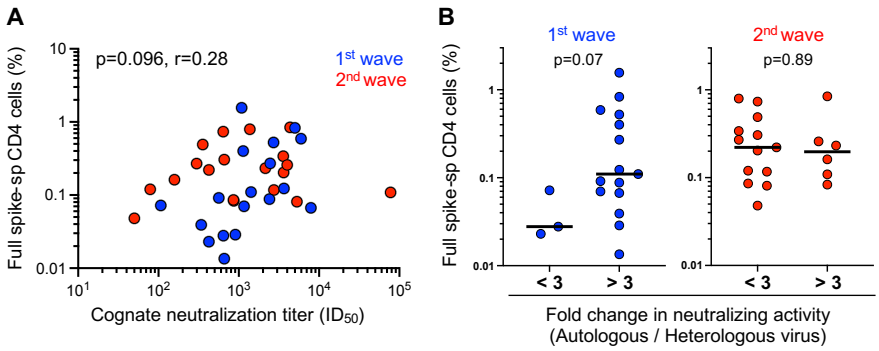

Fig. S3. Relationship between SARS-CoV-2-specific CD4 T cell responses and neutralizing activity. (A) Correlation between the frequency of ancestral SARS-CoV-2Spike-specific CD4 T cells and neutralization titers against cognate virus in 1st and 2nd wave patients. The correlation was tested by a two-tailed non-parametric Spearman rank test. **(B)** Comparison of the magnitude of ancestral SARS-CoV-2 Spike-specific CD4 T cell responses in patients exhibiting a fold change <3 or >3 in neutralizing activity against heterologous virus. Statistical analyses were performed using the Mann-Whitney test.

Supplementary Figure S4

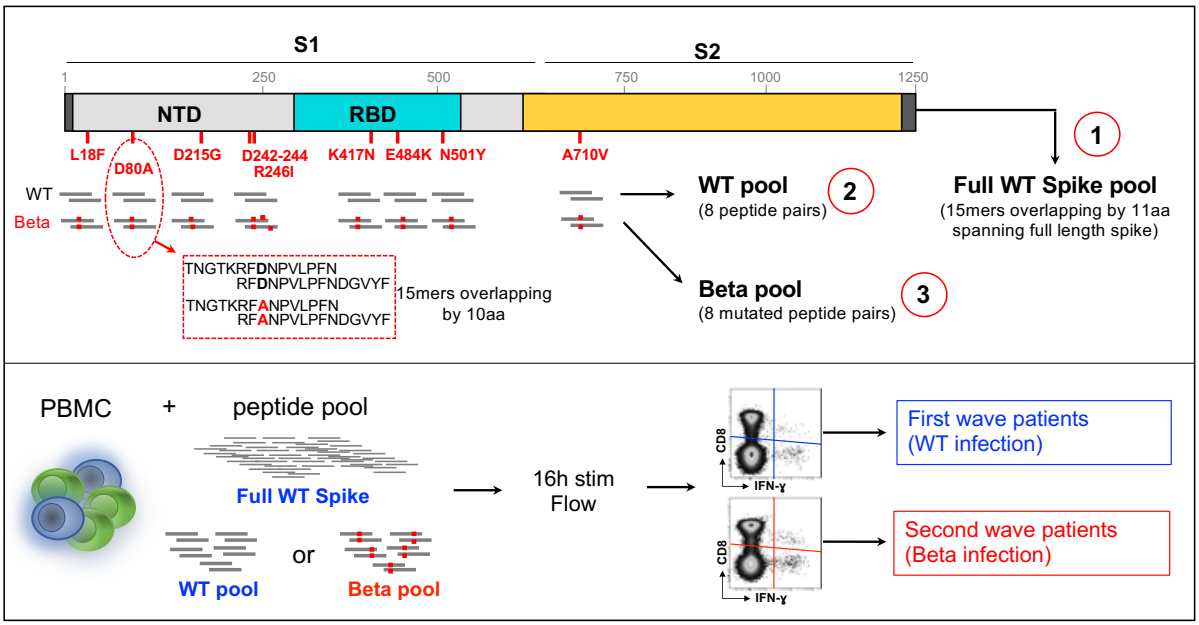

Fig. S4. Graphical representation of study approach. (A) SARS-CoV-2 Spike protein is depicted, demonstrating the design of ancestral and Beta variant peptides used in the immunological assays. **(B)** PBMC from patients recruited during the first or second wave of the pandemic in South Africa were stimulated with pools of peptides covering full Spike, or smaller pools spanning only the regions mutated in Beta, with wild type (WT) and corresponding mutated versions.

Supplementary Figure S5

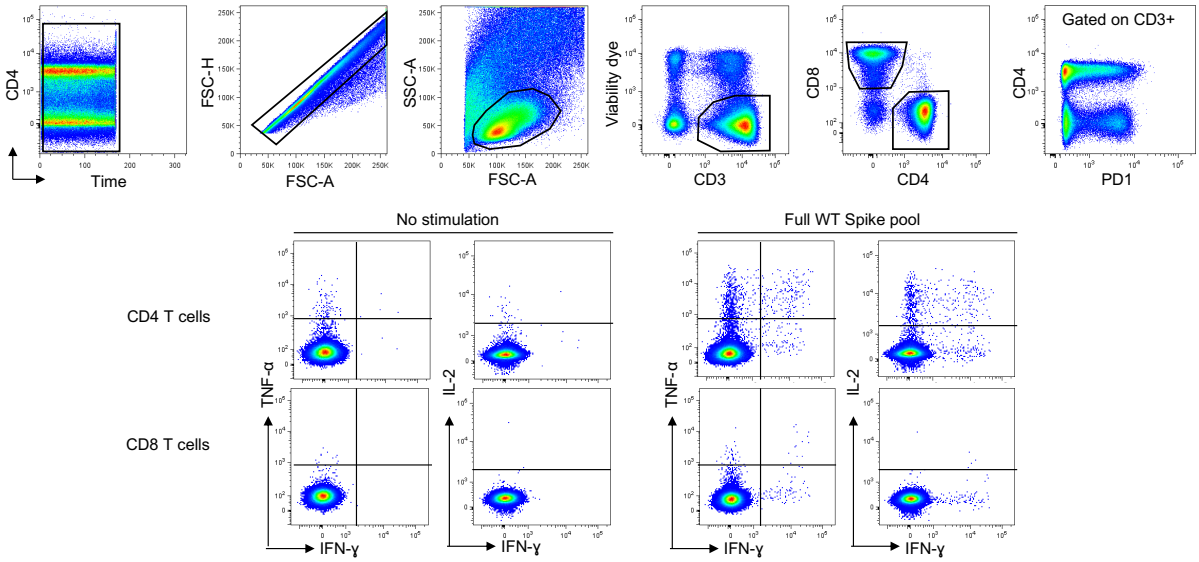

Fig. S5: Flow cytometry gating strategy. Representative example of flow cytometry staining profile and gating strategy.

Supplemental Table S1

Mutations of interest	Strain	Position aa (start)	Position aa (stop)	Sequence	Previously described
L18F	ancestral	6	20	VLLPLVSSQCVN<u>L</u>TT	Mateus et al.
L18F	ancestral	11	25	VSSQCVN<u>L</u>TTRTQLP	Tarke et al.
D80A	ancestral	73	87	TNGTKRF<u>D</u>NPVLPFN	
D80A	ancestral	78	92	RF<u>D</u>NPVLPFNDGVYF	Tarke et al.
D215G	ancestral	206	220	KHTPINLVR<u>D</u>LPQGF	Tarke et al.
D215G	ancestral	208	222	TPINLVR<u>D</u>LPQGFSA	Peng et al.
D215G	ancestral	211	225	NLVR<u>D</u>LPQGFSALEP	Peng et al.
242-244del/R246I	ancestral	236	250	TRFQTLLALH<u>R</u>SYLT	Mateus et al.
242-244del/R246I	ancestral	241	255	LLALH<u>R</u>SYLTPGDSS	Mateus et al.
K417N	ancestral	411	425	APGQTG<u>K</u>IADYNYKL	
K417N	ancestral	416	430	G<u>K</u>IADYNYKLPDDFT	Mateus et al.
E484K	ancestral	476	490	GSTPCNGV<u>E</u>GFNCYF	
E484K	ancestral	481	495	NGV<u>E</u>GFNCYFPLQSY	
N501Y	ancestral	492	506	LQSYGFQPT<u>N</u>GVGYQ	
N501Y	ancestral	496	510	GFQPT<u>N</u>GVGYQPYRV	
A701V	ancestral	701	715	<u>A</u>ENSVAYSNNSIAIP	Mateus et al.
L18F	Beta	6	20	VLLPLVSSQCVN<u>F</u>TT	
L18F	Beta	11	25	VSSQCVN<u>F</u>TTRTQLP	
D80A	Beta	73	87	TNGTKRF<u>A</u>NPVLPFN	
D80A	Beta	78	92	RF<u>A</u>NPVLPFNDGVYF	
D215G	Beta	206	220	KHTPINLVR<u>G</u>LPQGF	
D215G	Beta	208	222	TPINLVR<u>G</u>LPQGFSA	
D215G	Beta	211	225	NLVR<u>G</u>LPQGFSALEP	
242-244del/R246I	Beta	236	250	TRFQTLH<u>I</u>SYLTPGD	
242-244del/R246I	Beta	241	255	LH<u>I</u>SYLTPGDSSSGW	
K417N	Beta	411	425	APGQTG<u>N</u>IADYNYKL	
K417N	Beta	416	430	G<u>N</u>IADYNYKLPDDFT	
E484K	Beta	476	490	GSTPCNGV<u>K</u>GFNCYF	
E484K	Beta	481	495	NGV<u>K</u>GFNCYFPLQSY	
N501Y	Beta	492	506	LQSYGFQPT<u>Y</u>GVGYQ	
N501Y	Beta	496	510	GFQPT<u>Y</u>GVGYQPYRV	
A701V	Beat	701	715	<u>V</u>ENSVAYSNNSIAIP	

Table S1: List and sequence of 15-mer peptides contained in the ancestral (WT) and Beta peptide pools. References of previously described reactive peptides are provided in the last column. aa: amino acid. The site of mutations in Beta is underlined in the peptide sequence.

Supplemental Table S2

Mutations of interest	Strain	aa (start)	Sequence	Predicted HLA class II restriction
L18F	WT	6	VLLPLVSSQCVNLTT	DRB1*04:05, *15:01, *04:03
	Beta	6	VLLPLVSSQCVNFTT	DRB1*04:05, *15:01, *10:01
	WT	11	VSSQCVNLTTRTQLP	no match
	Beta	11	VSSQCVNFTTRTQLP	no match
D80A	WT	73	TNGTKRFDNPVLPFN	no match
	Beta	73	TNGTKRFANPVLPFN	no match
	WT	78	RFDNPVLPFNDGVYF	no match
	Beta	78	RFANPVLPFNDGVYF	no match
D215G	WT	206	KHTPINLVRDLPQGF	DRB1*03:01, *13:01, *13:02,
	Beta	206	KHTPINLVRGLPQGF	DRB1*11:04, *14:54, *04:03, *01:02, *11:01
	WT	208	TPINLVRDLPQGFSA	DRB1*03:01, *03:02, *13:01, *13:02, *14:54,
	Beta	208	TPINLVRGLPQGFSA	DRB1*11:04, *14:54, *08:04, *04:03, *01:02, *11:01
	WT	211	NLVRDLPQGFSALEP	DRB1*03:01, *13:02
	Beta	211	NLVRGLPQGFSALEP	DRB1*11:02
242-244del /R246I	WT	236	TRFQTLLALHRSYLT	DRB1*15:03, *12:02, *10:01, *14:24, *14:54, *01:01, *04:03, *15:01
	Beta	236	TRFQTLHISYLTPGD	DRB1*10:01, *01:01, *04:05, *07:01
	WT	241	LLALHRSYLTPGDSS	DRB1*15:01, *15:03, *07:01, *14:54, *14:25, *01:01
	Beta	241	LHISYLTPGDSSSGW	no match
K417N	WT	411	APGQTGKIADYNYKL	no match
	Beta	411	APGQTGNIADYNYKL	no match
	WT	416	GKIADYNYKLPDDFT	no match
	Beta	416	GNIADYNYKLPDDFT	no match
E484K	WT	476	GSTPCNGVEGFNCYF	no match
	Beta	476	GSTPCNGVKGFNCYF	no match
	WT	481	NGVEGFNCYFPLQSY	DQB1*05:02, DPB1*02:01
	Beta	481	NGVKGFNCYFPLQSY	DQB1*05:01, DPB1*02:01, DRB1*15:01,
N501Y	WT	492	LQSYGFQPTNGVGYQ	DRB1*09:01, *07:01, *04:01
	Beta	492	LQSYGFQPTYGVGYQ	DRB1*09:01, *07:01, *10:01
	WT	496	GFQPTNGVGYQPYRV	no match
	Beta	496	GFQPTYGVGYQPYRV	no match
A701V	WT	701	AENSVAYSNNSIAIP	DQB1*03:19, *03:01, DRB1*13:02, *04:01
	Beta	701	VENSVAYSNNSIAIP	DQB1*03:19, *03:01, DRB1*13:02, *04:01

Table S2: List of CD4 T cell epitopes used in this study and their predicted HLA class II restriction(s). Putative HLA class II restrictions were inferred using the Immune Epitope Database (IEDB) analysis resource (http://tools.iedb.org/mhcii/), using the IEDB recommended 2.22 prediction method. Prediction analyses were performed using all HLA class II (DR, DP, DQ) expressed in the studied cohort.

Supplemental Table S3

Wave	PID	HLA-DRB1		HLA-DQB1		HLA-DPB1	
1	SA1-001 #	DRB1*08:01	DRB1*13:01	DQB1*04:02	DQB1*06:03	DPB1*04:01	DPB1*04:02
1	SA1-002 #	DRB1*09:01	DRB1*15:01	DQB1*03:03	DQB1*06:03	DPB1*04:02	DPB1*14:01
1	SA1-005	DRB1*03:01	DRB1*07:01	DQB1*02:01	DQB1*02:02	DPB1*105:01	DPB1*105:01
1	SA1-007	DRB1*04:05	DRB1*13:02	DQB1*03:02	DQB1*06:09	DPB1*02:01	DPB1*17:01
1	SA1-008	DRB1*04:05	DRB1*12:02	DQB1*03:01	DQB1*03:02	DPB1*04:01	DPB1*13:01
1	SA1-015 #$	DRB1*13:01	DRB1*13:02	DQB1*06:03	DQB1*06:04	DPB1*01:01	DPB1*03:01
1	SA1-026	DRB1*04:04	DRB1*07:01	DQB1*03:02	DQB1*03:03	DPB1*04:01	DPB1*105:01
1	SA1-030	DRB1*11:01	DRB1*15:01	DQB1*03:01	DQB1*06:02	DPB1*04:01	DPB1*11:01
1	SA1-032 #	DRB1*13:03	DRB1*15:03	DQB1*06:02	DQB1*06:09	DPB1*02:02	DPB1*02:02
1	SA1-035 #$	DRB1*03:02	DRB1*12:01	DQB1*04:02	DQB1*05:01	DPB1*01:01	DPB1*131:01
1	SA1-043	DRB1*11:04	DRB1*11:14	DQB1*03:03	DQB1*03:03	DPB1*01:01	DPB1*105:01
1	SA1-049	DRB1*11:01	DRB1*11:01	DQB1*06:02	DQB1*06:02	DPB1*104:01	DPB1*104:01
1	SA1-066	DRB1*07:01	DRB1*08:04	DQB1*03:03	DQB1*04:02	DPB1*13:01	DPB1*105:01
1	SA1-068	DRB1*07:01	DRB1*11:01	DQB1*02:02	DQB1*06:02	DPB1*01:01	DPB1*02:01
1	SA1-075 #	DRB1*03:02	DRB1*15:01	DQB1*04:02	DQB1*06:01	DPB1*01:01	DPB1*02:01
1	SA1-087 #	DRB1*01:01	DRB1*04:03	DQB1*03:02	DQB1*05:01	DPB1*02:01	DPB1*04:02
1	SA1-090 #$	DRB1*12:02	DRB1*13:01	DQB1*03:01	DQB1*06:03	DPB1*02:01	DPB1*31:01
1	SA1-096 #$	DRB1*11:01	DRB1*14:54	DQB1*06:02	DQB1*06:02	DPB1*55:01	DPB1*104:01
1	SA1-098 #	DRB1*07:01	DRB1*14:25	DQB1*03:01	DQB1*03:03	DPB1*03:01	DPB1*04:01
1	SA1-099 #	DRB1*03:02	DRB1*11:02	DQB1*04:02	DQB1*06:09	DPB1*01:01	DPB1*01:01
1	SA1-155 #$	DRB1*10:01	DRB1*13:01	DQB1*05:01	DQB1*06:03	DPB1*02:01	DPB1*15:01
1	SA1-156	DRB1*04:03	DRB1*11:01	DQB1*03:01	DQB1*03:02	DPB1*04:01	DPB1*04:01
1	SA1c-004 #$	DRB1*03:01	DRB1*11:02	DQB1*02:01	DQB1*03:01	DPB1*02:01	DPB1*105:01
2	SA2-002	DRB1*01:02	DRB1*13:01	DQB1*05:01	DQB1*06:03	DPB1*03:01	DPB1*105:01
2	SA2-003	DRB1*08:04	DRB1*12:01	DQB1*03:01	DQB1*03:19	DPB1*02:01	DPB1*105:01
2	SA2-006	DRB1*07:01	DRB1*15:01	DQB1*03:03	DQB1*05:02	DPB1*03:01	DPB1*13:01
2	SA2-011	DRB1*15:01	DRB1*15:03	DQB1*06:01	DQB1*06:02	DPB1*01:01	DPB1*02:01
2	SA2-012	DRB1*12:01	DRB1*15:01	DQB1*05:01	DQB1*06:01	DPB1*02:01	DPB1*105:01
2	SA2-013	DRB1*07:01	DRB1*15:01	DQB1*02:01	DQB1*06:01	DPB1*04:01	DPB1*105:01
2	SA2-016	DRB1*07:01	DRB1*10:01	DQB1*02:02	DQB1*05:01	DPB1*04:01	DPB1*17:01
2	SA2-017	DRB1*03:01	DRB1*08:04	DQB1*02:01	DQB1*03:19	DPB1*105:01	DPB1*105:01
2	SA2-020 #	DRB1*13:01	DRB1*15:01	DQB1*06:02	DQB1*06:03	DPB1*04:01	DPB1*05:01
2	SA2-024	DRB1*07:01	DRB1*12:02	DQB1*02:02	DQB1*05:02	DPB1*04:01	DPB1*131:01
2	SA2-029 #	DRB1*07:01	DRB1*12:02	DQB1*03:01	DQB1*03:03	DPB1*05:01	DPB1*09:01
2	SA2-037	DRB1*15:03	DRB1*15:03	DQB1*06:02	DQB1*06:02	DPB1*01:01	DPB1*02:01
2	SA2-042	DRB1*11:01	DRB1*13:01	DQB1*03:19	DQB1*05:01	DPB1*01:01	DPB1*13:01
2	SA2-043	nd	nd	nd	nd	nd	nd
2	SA2-052	DRB1*03:02	DRB1*10:01	DQB1*04:02	DQB1*05:01	DPB1*01:01	DPB1*01:01
2	SA2-056	nd	nd	nd	nd	nd	nd
2	SA2-070	nd	nd	nd	nd	nd	nd
2	SA2-084	DRB1*03:01	DRB1*04:07	DQB1*02:01	DQB1*03:02	DPB1*02:01	DPB1*105:01
2	SA2-094 #	DRB1*10:01	DRB1*13:01	DQB1*05:01	DQB1*06:03	DPB1*03:01	DPB1*04:01
2	SA2-095	DRB1*10:01	DRB1*10:01	DQB1*04:02	DQB1*05:01	DPB1*01:01	DPB1*01:01
2	SA2-100	DRB1*11:01	DRB1*13:03	DQB1*03:01	DQB1*03:19	DPB1*01:01	DPB1*835:01
2	SA2-102	DRB1*13:01	DRB1*13:02	DQB1*06:09	DQB1*06:09	DPB1*18:01	DPB1*18:01

Table S3: HLA class II genotype (DRB1, DQB1 and DPB1) of acute COVID-19 patients.
[#]: Patients with a detectable CD4 T cell response to WT pool, [$]: Patients tested for identification of epitopes. nd: not done.

Supplemental Table S4

Wave	Donor ID	Epitope response (ICS)	Potential response (HLA prediction)	HLA-DRB1		HLA-DQB1		HLA-DPB1	
1	SA1-090	D215		DRB1*12:02	DRB1***13:01**	DQB1*03:01	DQB1*06:03	DPB1*02:01	DPB1*31:01
1	SA1-155	D215		DRB1*10:01	DRB1***13:01**	DQB1*05:01	DQB1*06:03	DPB1*02:01	DPB1*15:01
1	SA1c-004	D215		DRB1***03:01**	DRB1*11:02	DQB1*02:01	DQB1*03:01	DPB1*02:01	DPB1*105:01
1	SA1-015	D215/L18		DRB1***13:01**	DRB1*13:02	DQB1*06:03	DQB1*06:04	DPB1*01:01	DPB1*03:01
1	SA1-035	D215/L18		DRB1***03:02**	DRB1*12:01	DQB1*04:02	DQB1*05:01	DPB1*01:01	DPB1*131:01
1	SA1-096	D80		DRB1*11:01	DRB1*14:54	DQB1*06:02	DQB1*06:02	DPB1*55:01	DPB1*104:01
1	SA1-075	nd	D215/R246	DRB1***03:02**	DRB1***15:01**	DQB1*04:02	DQB1*06:01	DPB1*01:01	DPB1*02:01
1	SA1-001	nd	D215	DRB1*08:01	DRB1***13:01**	DQB1*04:02	DQB1*06:03	DPB1*04:01	DPB1*04:02
1	SA1-099	nd	D215	DRB1***03:02**	DRB1*11:02	DQB1*04:02	DQB1*06:09	DPB1*01:01	DPB1*01:01
1	SA1-002	nd	R246	DRB1*09:01	DRB1***15:01**	DQB1*03:03	DQB1*06:03	DPB1*04:02	DPB1*14:01
1	SA1-032	nd	R246	DRB1*13:03	DRB1***15:03**	DQB1*06:02	DQB1*06:09	DPB1*02:02	DPB1*02:02
1	SA1-087	nd	R246	DRB1***01:01**	DRB1*04:03	DQB1*03:02	DQB1*05:01	DPB1*02:01	DPB1*04:02
1	SA1-098	nd	R246	DRB1*07:01	DRB1***14:25**	DQB1*03:01	DQB1*03:03	DPB1*03:01	DPB1*04:01
2	SA2-020	nd	?	DRB1*13:01	DRB1*15:01	DQB1*06:02	DQB1*06:03	DPB1*04:01	DPB1*05:01
2	SA2-029	nd	?	DRB1*07:01	DRB1*12:02	DQB1*03:01	DQB1*03:03	DPB1*05:01	DPB1*09:01
2	SA2-094	nd	?	DRB1*10:01	DRB1*13:01	DQB1*05:01	DQB1*06:03	DPB1*03:01	DPB1*04:01

Table S4. List of Spike epitopes tested and their predicted HLA Class II restriction. Red corresponds to D215 restriction and green to R246 restriction.

Supplemental Table S5

Wave	Donor ID	HLA-A		HLA-B		HLA-C	
1	SA1-001	A*02:01	A*32:01	B*27:05	B*44:02	C*02:02	C*05:01
1	SA1-002	A*02:01	A*24:07	B*40:01	B*52:01	C*03:04	C*12:02
1	SA1-005	A*01:01	A*03:01	B*15:10	B*81:01	C*03:04	C*18:01
1	SA1-007	A*29:01	A*30:02	B*18:01	B*58:01	C*07:04	C*07:18
1	SA1-008	A*24:07	A*74:01	B*15:03	B*27:06	C*02:10	C*03:04
1	SA1-015	A*02:01	A*34:02	B*07:02	B*44:03	C*04:01	C*07:02
1	SA1-026	A*11:01	A*32:106	B*44:03	B*56:01	C*01:02	C*02:10
1	SA1-030	A*11:01	A*32:01	B*07:02	B*35:03	C*04:01	C*07:02
1	SA1-032	A*29:01	A*30:02	B*07:02	B*18:01	C*07:02	C*07:04
1	SA1-035	A*29:02	A*68:02	B*15:10	B*42:01	C*03:04	C*17:01
1	SA1-043	A*02:01	A*03:01	B*15:01	B*35:02	C*04:01	C*04:01
1	SA1-049	A*03:01	A*68:02	B*15:10	B*15:10	C*08:04	C*08:04
1	SA1-066	A*01:01	A*11:01	B*27:06	B*57:01	C*03:04	C*06:02
1	SA1-068	A*24:02	A*30:02	B*18:01	B*44:03	C*07:04	C*07:06
1	SA1-075	A*02:01	A*68:01	B*40:06	B*42:01	C*15:02	C*17:01
1	SA1-087	A*24:02	A*24:07	B*07:02	B*52:01	C*07:02	C*12:02
1	SA1-090	A*24:02	A*34:01	B*18:01	B*40:06	C*07:04	C*12:02
1	SA1-096	A*43:01	A*68:02	B*15:10	B*58:02	C*06:02	C*08:04
1	SA1-098 #	A*24:02	A*33:03	**B*35:05**	B*52:01	C*04:01	C*12:02
1	SA1-099	A*03:01	A*68:02	B*18:01	B*52:01	C*05:01	C*16:01
1	SA1-155	A*02:01	A*29:01	B*07:05	B*44:02	C*05:01	C*15:05
1	SA1-156	A*03:01	A*11:01	B*35:03	B*52:01	C*04:10	C*12:03
1	SA1c-004	A*01:01	A*68:01	B*08:01	B*58:02	C*06:02	C*07:01
2	SA2-002	A*02:01	A*30:01	B*42:02	B*57:03	C*07:01	C*17:01
2	SA2-003	A*02:131	A*30:01	B*07:06	B*15:10	C*03:04	C*07:02
2	SA2-006	A*11:01	A*32:01	B*07:06	B*57:01	C*06:02	C*07:02
2	SA2-011	A*02:03	A*68:02	B*14:02	B*38:02	C*07:02	C*08:02
2	SA2-012	A*02:11	A*36:01	B*13:02	B*40:06	C*06:02	C*15:02
2	SA2-013	A*26:12	A*33:03	B*40:06	B*58:02	C*06:02	C*15:02
2	SA2-016 #	A*02:05	A*02:05	B*50:01	**B*53:01**	C*06:02	C*06:02
2	SA2-017	A*02:01	A*02:02	B*18:01	B*53:01	C*04:01	C*05:01
2	SA2-020	A*01:01	A*26:01	B*38:01	B*41:02	C*12:03	C*17:03
2	SA2-024	A*03:01	A*11:01	B*35:30	B*58:02	C*04:01	C*06:02
2	SA2-029	A*02:01	A*31:01	B*15:08	B*15:03	C*01:02	C*08:01
2	SA2-037	A*24:02	A*68:02	B*07:02	B*13:02	C*06:02	C*07:02
2	SA2-042	A*02:01	A*03:01	B*14:02	B*15:03	C*02:10	C*08:02
2	SA2-043	nd	nd	nd	nd	nd	nd
2	SA2-052	A*34:02	A*68:02	B*15:10	B*44:03	C*03:04	C*04:01
2	SA2-056	nd	nd	nd	nd	nd	nd
2	SA2-070	nd	nd	nd	nd	nd	nd
2	SA2-084 #	A*23:01	A*24:07	**B*35:05**	B*58:01	C*04:01	C*07:18
2	SA2-094	A*11:01	A*11:01	B*44:03	B*52:01	C*04:01	C*12:02
2	SA2-095	A*02:81	A*29:02	B*15:10	B*42:01	C*03:04	C*17:01
2	SA2-100	A*01:01	A*03:01	B*15:16	B*81:01	C*14:02	C*18:01
2	SA2-102	A*02:01	A*30:02	B*39:10	B*44:03	C*07:06	C*12:03

Table S5: HLA class I genotype (HLA-A, -B and -C) of COVID-19 patients.
[#]: Patients with a detectable CD8 T cell response to the WT and Beta pools.

List of members of the South African cellular immunity network (SA-CIN)

Fatima Abrahams[1], Frances Ayres[2], Elloise du Toit[3], Rene T. Goliath[1], Willem Hanekom[4], Diana Hardie[3], Nei-Yuan Hsiao[3], Henrik Kloverpris[4], Stephen Korsman[3], Francisco Lakay[1], Bronwen Lambson[2], Alasdair Leslie[4], Zanele Makhado[2], Moepeng Maseko[3], Donald Mhlanga[2], Michelle Naidoo[3], Zaza Ndhlovu[4], Amkele Ngomti[3], Brent Oosthuysen[2], Sheena Ruzive[1], Alex Sigal[4], Tamryn Smith[3], Ziyaad Valley-Omar[3], Dieter van der Westhuizen[5], Kennedy Zvinairo[1]

[1]Wellcome Centre for Infectious Diseases Research in Africa, University of Cape Town; Observatory 7925, South Africa
[2]National Institute for Communicable Diseases of the National Health Laboratory Services; Johannesburg, South Africa
[3]Division of Medical Virology, Department of Pathology, University of Cape Town; Observatory 7925, South Africa
[4]Africa Health Research Institute; Durban, South Africa
[5]Division of Chemical Pathology, Department of Pathology, University of Cape Town; Observatory 7925, South Africa